AD-A082 215 TORONTO UNIV DOWNSVIEW (ONTARIO) INST FOR AEROSPACE --ETC F/G 20/9
STUDY OF LASER CREATED METAL VAPOR PLASMAS.(U)
NOV 79 R M MEASURES AFOSR-76-2902
UNCLASSIFIED AFOSR-TR-80-0193 NL

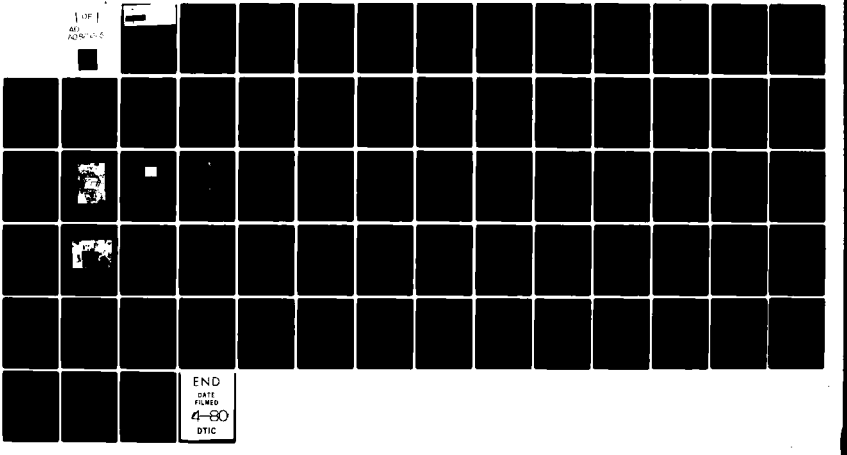

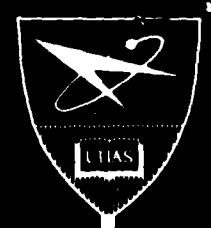

INSTITUTE
FOR
AEROSPACE STUDIES

UNIVERSITY OF TORONTO

AFOSR-TR- 80-0193

LEVEL II

(2)

A STUDY OF LASER CREATED METAL VAPOR PLASMAS

Final Technical Report

(for period ending September 30, 1979)

US AFOSR 76-2902

Prepared by

Dr. R. M. Measures
Professor of Applied Science and Engineering
Institute for Aerospace Studies
University of Toronto
4925 Dufferin Street
Downsview, Ontario, Canada
M3H 5T6

Unclassified

SECURITY CLASSIFICATION OF THIS PAGE (When Data Entered)

REPORT DOCUMENTATION PAGE	READ INSTRUCTIONS BEFORE COMPLETING FORM
1. REPORT NUMBER: AFOSR-TR-80-0193	2. GOVT ACCESSION NO. / 3. RECIPIENT'S CATALOG NUMBER
4. TITLE (and Subtitle): STUDY OF LASER CREATED METAL VAPOR PLASMAS	5. TYPE OF REPORT & PERIOD COVERED: Final Technical Report Oct. 1/78-Sept.30/79
	6. PERFORMING ORG. REPORT NUMBER
7. AUTHOR(s): Dr R. M. Measures	8. CONTRACT OR GRANT NUMBER(s): AFOSR-76-2902
9. PERFORMING ORGANIZATION NAME AND ADDRESS: University of Toronto, Institute for Aerospace Studies, 4925 Dufferin St., Downsview, Ontario, Canada, M3H 5T6	10. PROGRAM ELEMENT, PROJECT, TASK AREA & WORK UNIT NUMBERS: 61102F 2301/A7
11. CONTROLLING OFFICE NAME AND ADDRESS: Air Force Office of Scientific Research/NP Bldg. 410, Bolling Air Force Base, D.C. 20332, U.S.A.	12. REPORT DATE: Nov 1979 / 13. NUMBER OF PAGES: 68
14. MONITORING AGENCY NAME & ADDRESS(if different from Controlling Office)	15. SECURITY CLASS. (of this report): Unclassified / 15a. DECLASSIFICATION/DOWNGRADING SCHEDULE

16. DISTRIBUTION STATEMENT (of this Report)

Approved for public release; distribution unlimited.

17. DISTRIBUTION STATEMENT (of the abstract entered in Block 20, if different from Report)

18. SUPPLEMENTARY NOTES

19. KEY WORDS (Continue on reverse side if necessary and identify by block number)

X-Ray Laser, Laser Ablation Plasma, Metal Plasmas, Selective Excitation, Laser Ionization, Resonance Saturation, Inverse Bremsstrahlung, Laser Diagnostics, Plasma Heating, Laser Produced Plasmas, Associative Ionization, Multiphoton Ionization, Electron Temperature, Superelastic Collision Heating.

20. ABSTRACT (Continue on reverse side if necessary and identify by block number)

During the past year the "Laser Ablation and Selective Excitation Spectroscopy" facility has been extended to provide a dual wavelength excitation and monitoring capability. Work on an experiment, that is directed at making the first direct spatially and temporally resolved measurements of the ion to neutral ground state population ratio in a laser ablation plasma, has recently been commenced. The preliminary results attained to date have been encouraging.

Continued

DD FORM 1473 EDITION OF 1 NOV 65 IS OBSOLETE

In regard to the "Laser Interaction Based on Resonance Saturation" program advances have been made on three fronts: (i) A comprehensive study of the various seed electron creation processes has been undertaken. In the case of sodium vapour at 0.1 torr associative ionization has been shown to dominate two photon ionization of the resonance level for a laser irradiance below 10^7 W cm^{-2}. (ii) A simple model that is capable of predicting the ionization time analytically, under a wide range of conditions, has been developed. (iii) Electron superelastic collisions have been shown to lead to plasma heating rates in excess of 10^{13}°K sec^{-1} for modest values of laser irradiance.

(2)

CONTENTS

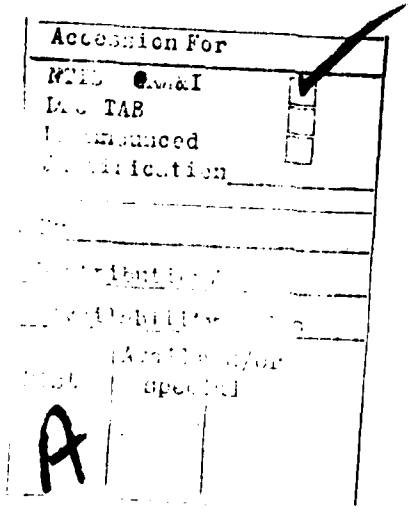

Officer

RESEARCH OBJECTIVES

The central theme of our current research program can be summarized as Laser Atom Selective Excitation (LASE), with an emphasis on those aspects that might have a bearing on the development and optimization of short wavelength lasers.

Short pulse lasers tuned to momentarily saturate specific transitions within atoms or ions make possible the measurement of atomic parameters (such as: radiative lifetimes, branching ratios and thereby transition probabilities) or the plasma conditions, depending upon the plasma density.[1-4] Extended laser saturation, on the other hand, perturbs the plasma and, in the case of resonance saturation, eventually leads to almost complete ionization burn-out of the species involved.[5-9] Our activities encompass both regimes.

The combination of laser ablation and selective excitation spectroscopy (LASES) leads in principle to a powerful laboratory technique for studying a variety of plasma conditions and species including short lived ions that are of interest in the development of X-ray lasers. Although our present LASES facility is limited to low states of ionization - due to the energy and wavelength of our lasers - we hope to demonstrate the basic principles and develop the techniques which when applied to more highly ionized species would yield information that could help in the optimization of short wavelength lasers. Our first attempts at this have included: measurements of radiative lifetimes, demonstrating metastable state freeze-out and mapping the distribution of a minor species in a rapidly expanding, laser ablated plasma. Currently we are about to embark upon a study of excited states within ionized species and demonstrate the ability of our technique to map the spatial and temporal distribution of such ionized species.

The idea of coupling laser energy to a gaseous medium through resonance saturation was first suggested by the author in 1970 in relation to MHD power generation.[5] The high efficiency of this interaction derives from the fact that the laser radiation is absorbed by a strong transition and is then readily transferred tothe free electrons through superelastic collisional quenching of the resonance level. In this way each atom is able to funnel many quanta of laser energy into the free electrons even in a brief period. Rapid ionization results from both the subsequent elevated electron temperature and the effective reduction of the ionization energy for those atoms pumped by the laser into the resonance state.

This LIBORS (laser interaction based on resonance saturation) concept lay dormant for 6 years until Lucatorto and McIlrath (in 1976) reported a surprising observation - sodium vapor at about 1 torr was almost completely ionized when irradiated with a 500 nsec pulse of laser radiation tuned to the 589.6 nm resonance line.[8] Lucatorto and McIlrath did not have a good explanation at the time, but by 1977 they had repeated their experiments with lithium and found the same rapid and almost complete ionization.[9] Geltman,[10] Lucatorto and McIlrath,[9] Bearman and Leventhal[11] and the author[6] independently proposed that the most plausible explanation for such an efficient and rapid ionization lay in a combination of the LIBORS concept and some trigger mechanism for initially creating free electrons. Multiphoton ionization seems the most likely candidate for some atoms, while in others associative ionization may dominate.

This rekindled interest in the LIBORS concept prompted us to undertake a comprehensive theoretical study of the interaction. Our analysis to date has revealed the effectiveness of LIBORS in heating and ionizing a gaseous or plasma medium.[6,12] Indeed, we have shown that the rate of laser energy deposition via LIBORS can exceed that through inverse bremsstrahlung by several orders of magnitude.[12] Put another way, a laser with an irradiance of 10^6 W cm^{-2} can achieve the same heating rate, through resonance saturation and electron superelastic collision quenching, as one with an irradiance of 10^{11} W cm^{-2} via inverse bremsstrahlung.

Stimulated emission at short wavelengths has been obtained through the use of rapid discharges in gases that have transitions that terminate on relatively long lived excited states.[13-15] Bristow et al[16] have suggested that this approach could be extended down to X-ray wavelengths through the use of very fast laser generated plasmas. We have recently undertaken calculations that indicate heating rates in excess of 10^{13} °K sec^{-1} could be achieved through superelastic laser energy conversion (SELEC) via resonance saturation of suitable ions.[17] Furthermore, this extremely fast plasma heating can be attained at modest laser irradiances and thereby avoiding the creation of superthermal runaway electrons. The ramifications of this work to X-ray laser development are obvious and could be of particular interest once optimization considerations are deemed important.

It may be helpful at this point to clarify the difference between SELEC and LIBORS, as both involve laser saturation of a resonance transition.

SELEC refers to the rapid electron heating that occurs prior to an appreciable increase in the free electron density, whereas LIBORS refers to the entire interaction that includes close to complete burn-out of the particular ion species being excited.

One of the formidable problems facing both the electron and ion beam approaches to inertial fusion is beam transportation across the reactor chamber to the fuel pellet. To facilitate the transportation of these focussed beams of charged particles, narrow plasma channels several meters in length will have to be created.[18-20] We have undertaken some extensive calculations that reveal that LIBORS should be particularly well suited for this purpose.[7]

Although the current LIBORS activity has been confined to first stage ionization of alkali metal vapors, the development of short wavelength lasers and the use of multiphoton saturation should enable the LIBORS concept to be applied to a wide range of elements and stages of ionization. Furthermore, at the high densities found in laser ablated plasmas, the time to burn out a given state of ionization would be reduced to the subnanosecond scale. Consequently, we view LIBORS to be a possible new method of efficiently and rapidly coupling laser energy into the kind of laser ablated plasma that is likely to constitute the medium for X-ray laser generation.

We plan to undertake a comprehensive study aimed at obtaining a better understanding of LIBORS and demonstrating its advantages. This program will include an expanded theoretical and computational study coupled to a new experimental investigation.

An overview of our two programs is presented as figure 1.

STATUS OF RESEARCH

LASES-Program

Our LASES facility has undergone a major redesign and improvement during the past year. We now have two nitrogen laser pumped dye lasers and a dual wavelength photodetection system. We have a new low pressure ablation chamber that has six optical ports and a rotatable multi-sample target that allows us to undertake many experiments without breaking the system's vacuum. A Q-switched ruby laser is still used to create the ablation plasma. An overview of the facility is presented as figure 2. A closeup of the new

ablation chamber and improved photodetection system is shown in the foreground An RCA C31034 PMT and a SPEX 1700 monochromator is used in one channel, while an RCA 4526 PMT and a Jobin-Yvon H20 monochromator is used in the other channel.

Lifetime Measurements

As a demonstration of our LASES approach to the measurement of atomic parameters we initially evaluated the radiative lifetime of the three resonance transitions of chromium[4] and have extended these measurements to situations where the chromium was only a trace constituent of the ablated material. This showed that lifetime measurements of minor species of the plasma could be evaluated and at the same time suggested a new kind of ultrasensitive trace element laser microprobe.[21,22] We have recently commenced a new series of experiments that will involve the measurement of radiative lifetimes of excited states in the ions that are created within the ablation plasma. Of special interest will be states that are excited by stepwise two photon pumping.

Although this information may not be immediately applicable to X-ray laser development at this stage, we are laying the foundations of techniques that will provide relevant information when undertaken with shorter wavelength probe lasers and more powerful ablation lasers.

Ablation Plasma Studies

Recently we have initiated a new project that is aimed at testing the diagnostic capability of the selective excitation spectroscopy concept first proposed by the author.[1] (See Appendix A for an updated review.) In this instance the ratio of laser intensified spontaneous emission arising from the neutral and ion resonance state will be evaluated in an attempt to map the temporal variation in the degree of ionization of a specific constituent within a rapidly expanding, laser ablation plasma. Strontium has been selected for this preliminary work since both the neutral and singly ionized form possess resonance line wavelengths (Sr I 460.7 and Sr II 421.6 nm) that fall within the operating range of our present dye lasers.

Within the past few weeks we have undertaken some preliminary experiments that have assured us of the viability of this project. In particular, the strength of the intensified emission signals from both the neutral and

ionic species appears satisfactory as can be seen by reference to figure 3. The upper trace corresponds to the intensified spontaneous emission (ISE) signal that stems from the strontium atoms within a small volume* located about 1 cm from the strontium doped target. The lower trace corresponds to the ISE signal that originates from the strontium ions within the same volume and at the same instant of time. The poor quality of the ion ISE signal is due to a weak laser pulse. The cause of this low output is known and is being corrected. Although the literature is rich with references to observations of the motion of ions and electrons expanding from laser ablation plasmas, our direct comparison of neutrals to ions for a given species will be new.

It might be noted in passing that in last year's measurement of metastable freeze out of chromium atoms, the two transitions had to be sequentially excited since we only had one photodetector and one single beam fast oscilloscope. Our new facility has two, wavelength independent, photodetection channels and a new fast dual beam oscilloscope.

LIBORS - Theoretical Program

Over the past two years we have developed both a comprehensive computer code and a relatively simple model for studying LIBORS. The LIBORS computer code treats the atom as a 20 energy level system and takes account of the important radiative-collisional processes. The corresponding set of population rate equations are solved simultaneously with the ionization equation, the free electron energy equation and the interspecies elastic energy transfer equations. The details of the LIBORS code will not be given here, but are presented in our publications.[7,12,23,24]

In essence the LIBORS code predicts the temporal behaviour of: the population in each of the energy levels, the free electron density and temperature, the ion temperature, the laser power absorbed and the recombination radiation - subsequent to sudden laser saturation of one of the species' resonance transitions. The LIBORS simple model will be discussed later and will be seen to offer considerable insight into the physical processes involved and provides a quick means of predicting, in a qualitative manner, the ionization time for any species. The basic processes involved are displayed in figure 4.

The advances made during the past year are summarized below:

*Defined by the dye laser beams and the common field of view of the photodetection system.

(1) Comparative Study of Seed Electron Creation Processes

In the case of an un-ionized gas, the energy stored in the laser saturated resonance state population can only be effectively tapped by free electrons, once free electrons exist. If near complete ionization is to be achieved within the duration of the laser pulse, a rapid means of creating the initial free electrons is mandatory. The three most likely seed processes in the case of sodium are:[24]

(i) Associative Ionization (A)

$$Na(3p) + Na(3p) \rightarrow Na_2^+ + e + KE \ (\approx 0.04 \text{ eV})$$

(ii) Laser-Induced Penning Ionization (LIP)

$$Na(3p) + Na(3p) + h\nu \rightarrow Na^+ + Na(3s) + e + KE \ (\approx 1.17 \text{ eV})$$

(iii) Resonance State Two Photon Ionization (RTP)

$$Na(3p) + 2h\nu \rightarrow Na^+ + e + KE \ (\approx 1.17 \text{ eV})$$

Na(3p) and Na(3s) represent a resonance and ground state atom, respectively. $h\nu$ represents a laser photon (equal to the resonance to ground state energy difference).

Although the seed electrons may be created with a small amount of kinetic energy (as indeed is the case for associative ionization), once freed, they rapidly acquire translational energy through superelastic collisions with the vast reservoir of laser maintained resonance state atoms. The free electron mean translational energy will quickly rise to a value that is determined by a balance between superelastic and inelastic collisions.[6,17,23]

Laser saturation of one of the resonance transitions leads, according to Measures,[1] to resonance level population density equal to GN_o, where $G = g_2/(g_2 + g_1)$, g_2 and g_1 being the resonance and ground level degeneracies, respectively, and N_o is the ground state atom density prior to laser irradiation. Consequently, the initial ionization rate resulting from associative ionization of laser saturated sodium vapor can be expressed in the form

$$\left.\frac{dN_e}{dt}\right|_A \approx \frac{9N_o^2}{32}\,\sigma_A \left\{\frac{8kT}{\pi m}\right\}^{1/2}$$

where σ_A is the appropriate cross section and $\{8kT/\pi m\}^{1/2}$ represents the mean velocity of the sodium atoms. Geltman[10] has estimated this cross

section to be about 10^{-17} cm^2 while Bearman and Leventhal[11] indicate a value closer to 10^{-15} cm^2 might be expected.

In the case of laser induced penning ionization, we can write

$$\left.\frac{dN_e}{dt}\right|_{LIP} \approx \frac{9N_o^2}{32}\,\sigma_{LIP}\,F\left\{\frac{8kT}{\pi m}\right\}^{1/2}$$

where $\tilde{\sigma}_{LIP} \equiv (\sigma_{LIP}F)$ is the appropriate cross section and F is the laser photon flux density ($F = I^{\ell}/h\nu$). In the case of the sodium D_1 line $\sigma_{LIP} \approx 4 \times 10^{-44}$ (cm^4s) according to Geltman[10] and Cardinal.[24]

The resonance state two photon ionization rate can for sodium be expressed in the form

$$\left.\frac{dN_e}{dt}\right|_{RTP} \approx \frac{3N_o}{16}\,\sigma_{2c}^{(2)}F^2$$

here, $\sigma_{2c}^{(2)}$ (cm^4s) is the appropriate rate coefficient. Cardinal[24] has estimated that in the case of sodium, $\sigma_{2c}^{(2)} \approx 1.7 \times 10^{-49}$ (cm^4s).

The dependence of the net initial ionization rate upon the laser irradiance (I^{ℓ}) is presented in figure 5 for the two possible associative ionization cross sections. In the case of sodium vapour, associative ionization is seen to dominate (even with the smaller cross section) the ionization rate for $I^{\ell} < 10^7$ W cm^{-2}. The right hand scale of figure 5 gives the effective time for the vapour to ionize if these three seed processes were the only ionization mechanisms.

Figure 6 indicates the operating regimes under which the different seed electron processes are comparable. The figure is divided into two sets of 6 zones (a, b, c, d, e, f or A, B, C, D, E, F) by the lines defining the equalities:

$$\left.\frac{dN_e}{dt}\right|_{A} = \left.\frac{dN_e}{dt}\right|_{LIP} \qquad \text{Lines } \alpha \text{ or } \alpha^*$$

$$\left.\frac{dN_e}{dt}\right|_{RTP} = \left.\frac{dN_e}{dt}\right|_{A} \qquad \text{Lines } \beta \text{ and } \beta^*$$

$$\left.\frac{dN_e}{dt}\right|_{LIP} = \left.\frac{dN_e}{dt}\right|_{RTP} \qquad \text{Lines } \gamma \text{ and } \gamma^*$$

The asterisked quantities relate to calculations using Geltman's[10] cross section for association ionization - the others to Bearman and Leventhal's[11] value. The operating conditions in the experiments of Lucatorto and McIlrath,[8] and assumed in our earlier calculations,[6,7,12] lie in region D (or d) where associative ionization is likely to be the dominant initial ionization process (provided $\sigma_A \gtrsim 2 \times 10^{-17}$ cm^2).

(2) Simple Model Representation of LIBORS

Consequently, we have had to allow for this process in both our LIBORS computer code and in our simple model representation of LIBORS. We have also included the influence of single photon ionization in both the code and the model. Our updated simple model is portrayed in figure 7 and leads to an ionization equation of the form

$$\frac{dN_e}{dt} = N_2 \left\{ \sigma_{2c}^2 F^2 + \frac{1}{2} N_2 v(\sigma_{IP} F + \sigma_A) \right\} + N_3 \sigma_p F + N_2 N_e K_{2c} + N_3 N_e K_{3c} \qquad (1)$$

where N_2 (cm^{-3}) represents the resonance level population density,
v (cms^{-1}) represents the mean thermal velocity of sodium atoms,
N_3 (cm^{-3}) represents the intermediate level population density,
σ_p (cm^2) represents the mean single photon ionization cross section for the intermediate level,
K_{nc} (cm^{3}s^{-1}) represents the electron collisional ionization rate coefficient for level n, and
N_e (cm^{-3}) represents the free electron density.

Notice the hierarchy of the processes, first the seed processes dominate as both N_e and N_3 are small, then as N_e builds such that the population in the intermediate levels become finite (due to inelastic excitation primarily from resonance level) single photon ionization starts to become important. Next direct electron collisional ionization of the resonance level and finally the last term which reflects the "ionization burn out phase" as the growth in the free electrons exceeds the exponential growth rate.

To solve for $N_e(t)$ we need to know how N_3 varies with time. In order to keep the model simple we shall assume that we can write the steady state equation

$$N_3 \approx N_2 N_e K_{23} \tau_3^* \qquad (2)$$

where $\tau_3^* = \tau_3 (1 + \sigma_p F \tau_3)^{-1}$, τ_3 being the spontaneous decay time of level 3. Under these circumstances the electron creation equation can be expressed in the form:

$$\frac{dN_e}{dt} = S + IN_e + BN_e^2 \qquad (3)$$

where $S \equiv N_2\{\sigma_{2c}^{(2)} F^2 + \frac{1}{2} N_2 v(\sigma_{LIP} F + \sigma_A)\}$ represents the seed processes,

$I \equiv N_2\{K_{2c} + K_{23}\sigma_p F \tau_3^*\}$ represents the intermediate processes, and

$B \equiv N_2 K_{23} K_{3c} \tau_3^*$ represents the burn-out processes.

It is assumed that S, I and B remain constant over the time interval required for the degree of ionization to reach about 1%. This is not too bad an approximation since $N_2 \approx GN_o$, for sudden laser saturation at $t = 0$, and N_o (the atom density) will only start to deviate from its original value once the degree of ionization exceeds 1%. Also, the temperature tends to stabilize very rapidly (in a time short compared to that required for ionization[23]).

Equation (3) has two forms of analytical solution depending on the relative values of S, I and B:

(i) If $I^2 < 4SB$, which corresponds to seed electron domination over the intermediate processes until electron collisional burn-out takes over, then under these circumstances the analytical form of the solution will be

$$t = \frac{2}{\sqrt{q}} \left[\tan^{-1} \left\{ \frac{2BN_e + I}{\sqrt{q}} \right\} - \tan^{-1} \left\{ \frac{I}{\sqrt{q}} \right\} \right] \qquad (4)$$

where $q \equiv 4SB - I^2$; and

(ii) If $I^2 > 4SB$, which corresponds to weak seed electron processes as well as to strong intermediate interactions, then the solution is

$$t = \frac{1}{\sqrt{Q}} \left[\ell n \left\{ \frac{2BN_e + I - \sqrt{Q}}{2BN_e + I + \sqrt{Q}} \right\} - \ell n \left\{ \frac{I - \sqrt{Q}}{I + \sqrt{Q}} \right\} \right] \qquad (5)$$

where $Q \equiv I^2 - 4SB$. For modest values[24] of photon flux density, F, we can simplify equation (5) by writing

$$\sqrt{Q} \approx I - \frac{2SB}{I}$$

This results in a simple equation for the time to reach a given electron density, viz.,

$$t \approx \frac{1}{I}\left[\ell n \left\{ \frac{I^2}{SB} \right\} + \ell n \left\{ 1 + \frac{S}{IN_e} \right\} - \ell n \left\{ 1 + \frac{I}{BN_e} \right\} \right] \qquad (6)$$

We can now introduce two characteristic electron densities:

(i) $N_e^* \equiv \frac{S}{I}$ represents the electron density for which the rate of ionization based upon seed electron processes equals the rate of ionization based upon intermediate processes; and

(ii) $N_e^{**} \equiv \frac{I}{B}$ represents the density for which the rate of ionization based upon the intermediate processes equals the direct electron collisional ionization of the third level.

This allows us to write equation (6) as follows:

$$t \approx \frac{1}{I}\left[\ell n \left\{ \frac{N_e^{**}}{N_e^*} \right\} + \ell n \left\{ 1 + \frac{N_e^*}{N_e} \right\} - \ell n \left\{ 1 + \frac{N_e^{**}}{N_e} \right\} \right] \qquad (7)$$

Although equation (7) is strictly valid only for a degree of ionization less than 1%, the steepness of the ionization curve towards the burn-out phase is such that negligible error is incurred by equating the ionization burn-out time τ_B to the limiting value of equation (7), namely

$$\tau_B \approx \frac{1}{I} \ell n(N_e^{**}/N_e^*) \qquad (8)$$

The sensitivity of the ionization burn-out time to the associative ionization cross section can be ascertained by reference to figure 8, where the growth of the free electron density, as given by equation (5), is presented for several values of σ_A.

(3) Improved LIBORS Computer Code Results

The LIBORS energy level scheme adopted for the sodium atom is presented as figure 9. This diagram clearly reveals that once laser saturation of the resonance level (we assume that the $3^2P_{3/2}$ and $3^2P_{1/2}$ spin states are

coalesced by collisions) occurs, collisional excitation to the higher levels leads to the possibility of direct single photon ionization by the laser radiation. The influence of this photoionization is clearly seen in figure 10, where the temporal variation in the resonance level population $N_2(3p)$, the electron density N_e, the electron temperature T_e and the ion temperature T_i, are shown for two situations; one where the photoionization cross section $\sigma_{pc}^{(1)} = 0$, the other where the values of $\sigma_{pc}^{(1)}$ are given by the quantum modified Kramer's formulae.[25]

In figure 11 we demonstrate the impact of associative ionization and laser induced penning ionization upon the temporal behaviour of N_2, N_e, T_e and T_i in the case of sodium vapor at about 0.1 torr. As stated earlier, however, associative ionization dominates laser induced penning ionization for the modest level of laser irradiance assumed in this LIBORS code simulation. It is worth noting that our LIBORS computer code predicts that the initial jump in the electron temperature is smaller when associative ionization is taken into account. This is a direct consequence of the very small excess energy of ionization involved in associative ionization in comparison with the other seed processes.

(4) Plasma Heating Through Superelastic Collisions

In general the superelastic heating rate for the free electrons, under conditions of resonance saturation, can be expressed in the form

$$Q^{SE} = N_e N_2 K_{21} E_{21}$$

We have shown[7,12] that the maximum rate of laser energy deposition via LIBORS arises just prior to "ionization burn-out" of the laser saturated species and, in the case of a neutral species, takes the form

$$Q^{\ell}_{max} = G N_o^2 K_{21} E_{21}/4 \qquad (Wcm^{-3})$$

where $G = g_2/(g_2+g_1)$,

g_2 and g_1 represent the respective degeneracies of the resonance and ground levels of the atom,

N_o represents the original atom number density prior to laser irradiation,

K_{21} the superelastic electron collision rate coefficient, and

E_{21} the laser photon energy (equal to the resonance to ground energy),

Q^{ℓ}_{max} is plotted as a function of N_o for sodium in figure 12.

A direct comparison with the rate of laser energy deposition through inverse bremsstrahlung, Q_{IB}, yields

$$H \equiv \frac{Q^{\ell}_{max}}{Q_{IB}} = \frac{3c^2(kT_e)^{3/2}GK_{21}E_{21}}{1.17 \times 10^{-7}\lambda^2 I^{\ell}}$$

where k, h and c have their usual value, I^{ℓ} represents the laser irradiance (Wcm^{-2}), T_e the free electron temperature (kT_e in eV). For the case of sodium vapor we can write [12]

$$H \approx \frac{1.5 \times 10^{11}}{I^{\ell}}$$

Clearly the rate of deposition of energy through LIBORS greatly exceeds that through inverse bremsstrahlung over a wide range of laser irradiance. Additional advantages possessed by LIBORS include: more efficient interaction, operates at much lower laser power levels, much shorter interaction length, linear attenuation of laser beam and cold (un-ionized) start capability even at modest laser power levels.

In general the maximum temperature T_c^{max} achieved through superelastic heating of a laser saturated resonance transition is determined by the characteristics of the laser pumped species. We have recently[17] developed a simple three level model of this interaction that enables us to characterize the maximum temperature attainable in terms of two parameters: the energy level ratio "a" and the superelastic to inelastic collision ratio "b". That is to say:

$$a \equiv E_{32}/E_{21} \qquad \text{and} \qquad b \equiv g_1\bar{f}_{12}/g_2\bar{f}_{23}$$

where E_{32} represents the energy gap between the resonance energy and the next level having a strong optical transition to the resonance level.

$\bar{f}_{nm}$ represents the product of the absorption oscillator strength and the effective mean Gaunt factor for the nm-transition.

If we introduce the normalized temperature, $\theta \equiv kT_e/E_{21}$, then the free electron energy equation for this simple three level model takes the form

$$\frac{d\theta}{dt} = \frac{2}{3} N_2 K_{21} \left[1 - \exp\{-1/\theta\} - \frac{1}{b} \exp\{-a/\theta\}\right]$$

The transcendental equation obtained by assuming steady state conditions has been solved and the results presented in figure 13. Reference to figure 13 leads to the conclusion that a substantial heating will be attained for those laser pumped species possessing as large a value as possible for both "a" and "b".

With this in mind boron III was selected as representative of a suitable ion. The partial energy level diagram for BIII is presented in figure 14. Our LIBORS code was adapted to the case of BIII, using the 14 levels shown in figure 14. In this instance we assumed that we started with a BIII plasma that was in local thermodynamic equilibrium so that our initial conditions could be described in terms of an initial electron temperature T_{eo}, such that the initial electron density could be equated (within 10%) to the initial BIII density.

The LIBORS code predicted temporal variation of the free electron temperature, subsequent to sudden laser saturation of the BIII resonance transition (at 206 nm), for three initial BIII densities is presented in figure 15. Of particular interest is the very fast heating rate indicated at the higher densities. For the highest density considered, $N(BIII) = 10^{17}$ cm^{-3}, a heating rate in excess of 4×10^{13} °K sec^{-1} is predicted for a modest laser irradiance of 10^8 W cm^{-2} in a 2 mm plasma.[17] This very high heating rate could be ideal for creating transient nonequilibrium distributions that are conducive to the development of short wavelength lasers.

LIBORS - Experimental Program

Although our LIBORS computer code is fairly comprehensive most of the collision cross sections are not known to an accuracy of better than a factor of 3 and some key cross sections like σ_A, $\sigma_{2c}^{(2)}$ and $\sigma_{pc}^{(1)}$ are even less well defined. In addition features such as: self focussing or coherency effects could modify the form and characteristics of the interaction and our present treatment does not include diffusion or the influence of spatial gradients. Consequently, we are in the process of building an experimental facility that will be used to investigate LIBORS and obtain experimental data that can be compared with our computer predictions, thereby strengthening our theoretical understanding of this interaction and placing us in a better position to gauge the applicability of LIBORS to various areas of endeavour.

In order to undertake the first time resolved measurements of laser ionization based on resonance saturation we built an experimental facility around a sodium vapour Pyrex cell that we had in our possession. An overview of the facility is presented in figure 16. It was recognized at the outset that this Pyrex cell may not be adequate for the job since it was never designed to be heated to a temperature sufficient to attain a vapour pressure of 0.1 torr of sodium vapour and even if it were to stand the temperature the speed of sodium deposition on the windows was an unknown.

The basic facility comprises: a flashlamp pumped dye laser that was tuned to the sodium D_1 resonance line and could deliver close to 1 MW cm^{-2} within the cell for about 600 nsec, a photodetection system that included a monochromator-photomultiplier combination for observing the laser produced plasma radiation and two photodiodes, PD1 and PD2, for monitoring the attenuation of the laser pulse. Two cameras were also used, C1 to record the far field of the transmitted laser radiation to observe for self focussing effects, and C2 which was to observe a broad band (as determined by the SPEX monochromator) of the plasma emission in an attempt to monitor the presence of filamentation. A schematic of this facility is presented as figure 17.

Figure 18 presents the LIBORS code predicted time history of the continuum radiation (arising from radiative recombination to the 3p resonance level) and the laser power absorbed under the experimental conditions anticipated within our initial LIBORS experiment.

Unfortunately, our concern in regard to the lifetime of the sodium vapour Pyrex cell turned out to be justified and no useful experimental data were obtained due to a major failure of the cell windows prior to

obtaining the desired operating conditions.

New LIBORS Facility

Currently, we are building a new heat cell that is based on the advanced design of Boyd et al.[26] This heat cell will enable excellent optical access to the interaction region and should certainly be adequate for our range of operating conditions. The remainder of the facility will more or less remain the same.

REFERENCES

1. R. M. Measures, J. Appl. Phys. 39, 5232-5245 (1968).
2. R. A. Stern and J. A. Johnson III, Phys. Rev. Lett. 34, 1548-1550 (1975).
3. A. B. Rodrigo and R. M. Measures, IEEE J. of Quant. Electr. QE-9, 972-978 (1973).
4. R. M. Measures, N. Drewell and H. S. Kwong, Phys. Rev. A 16, 1093-1097 (1977).
5. R. M. Measures, J. Quant. Spectrosc. Radiat. Transfer, 10, 107-125 (1970).
6. (a) R. M. Measures, J. Appl. Phys. 48, 2673-2675 (1977).
   (b) R. M. Measures, N. Drewell and P. Cardinal, "Radiation Energy Conversion in Space" (Ed. K. W. Billman), 450-464 (1978, Vol. 61 of Progress in Astronautics and Aeronautics.
7. R. M. Measures, N. Drewell and P. Cardinal, J. of Appl. Phys. 50, 2662-2669 (1979).
8. T. B. Lucatorto and T. J. McIlrath, Phys. Rev. Lett. 37, 428-431 (1976).
9. T. J. McIlrath and T. B. Lucatorto, Phys. Rev. Lett., 38, 1390-1393 (1977).
10. S. Geltman, J. Phys. B, 10, 3057 (1977).
11. G. H. Bearman and J. J. Leventhal, Phys. Rev. Lett., 41, 1227-1230 (1978).
12. R. M. Measures, N. Drewell and P. Cardinal, Appl. Optics, 18, 1824-1827 (1979).
13. R. T. Hodgson, Phys. Rev. Letters, 25, 494 (1970).
14. R. T. Hodgson and R. W. Dreyfus, Phys. Rev. Letters, 28, 533 (1972).
15. R. W. Waynant, Phys. Rev. Letters, 28, 536 (1972).
16. T. C. Bristow, M. J. Lubin, J. M. Forsyth, E. B. Goldman and J. M. Soures, Optics Commun. 5, 315-318 (1972).
17. R. M. Measures, P. L. Wizinowich, P. G. Cardinal, "Fast and Efficient Plasma Heating Through Superelastic Laser Energy Conversion (SELEC)" (Submitted to J. of Appl. Physics, 1979).
18. P. A. Miller, R. I. Butler, M. Cowan, J. R. Freeman, J. W. Poukey, T. P. Wright and G. Yonas, Phys. Rev. Letters, 39, 92-95 (1977).
19. T. P. Wright, J. Appl. Phys. 49, 3842-3850 (1978).
20. J. R. Freeman and J. W. Poukey, J. Appl. Phys. 50, 5691-5693 (1979).

21. R. M. Measures and H. S. Kwong, Appl. Optics, 18, 281-286 (1979).
22. H. S. Kwong and R. M. Measures, Analytical Chem., 51, 528-432 (1979).
23. N. Drewell, "Studies of Laser Selective Excitation of Atoms", UTIAS Report No. 229, 1979.
24. P. G. Cardinal (Unpublished).
25. G. V. Marr, "Photoionization Processes in Gases", Academic Press (1967).
26. J. G. Dodd, J. Krasinski, R. W. Boyd and C. Stroud, "Metal-Vapor Oven with 2π Radians Optical Access", Paper WB4, 1979 Annual Meeting of Optical Society of America.

CUMULATIVE CHRONOLOGICAL LIST OF PUBLICATIONS (1974-PRESENT)

1. R. M. Measures, P. L. Wizinowich, P. G. Cardinal, "Fast and Efficient Plasma Heating Through Superelastic Laser Energy Conversion (SELEC)" (Submitted to J. Appl. Phys., 1979)
2. R. M. Measures, N. Drewell, P. Cardinal, "Electron and Ion Beam Transportation Channel Formation by Laser Ionization Based on Resonance Saturation - LIBORS", J. Appl. Phys., 50, 2662-2669 (1979).
3. R. M. Measures, N. Drewell, P. Cardinal, "Laser Interaction Based on Resonance Saturation (LIBORS) - An Alternative to Inverse Bremsstrahlung for Coupling Laser Energy into a Plasma", Appl. Optics, 18, 1824-1827 (1979).
4. H. S. Kwong, R. M. Measures, "Trace Element Laser Microprobe Having High Sensitivity and Freedom from Chemical Matrix Effects", Analytical Chemistry, 51, 428-432 (1979).
5. R. M. Measures, H. S. Kwong, "Development of a Trace Element Analyser Based on Laser Ablation and Selective Excited Radiation - TABLASER", Appl. Optics, 18, 281-285 (1979).
6. R. M. Measures, N. Drewell, P. Cardinal, "Superelastic Laser Energy Conversion (SELEC)", Radiation Energy Conversion in Space (Ed. K. W. Billman), Vol. 61 of Progress in Astronautics and Aeronautics (1978).
7. R. M. Measures, "PROBE - Profile Resolution Obtained by Excitation", Applied Spectroscopy, 32, 381-388 (1978).
8. R. M. Measures, "PROBE - A New Technique for Measuring the Density Profile of a Specific Constituent Using Counter Propagating Laser Pulses", Appl. Optics, 16, 3016-3026 (1977).
9. R. M. Measures, N. Drewell, H. S. Kwong, "Atomic Lifetime Measurement Obtained by Use of Laser Ablation and Selective Excitation Spectroscopy", Phys. Rev. A, 16, 1093-1097 (1977).
10. R. M. Measures, "Efficient Laser Ionization of Sodium Vapor - A Possible Explanation Based on Superelastic Collisions and Reduced Ionization Potential", J. Appl. Phys., Vol. 48, 2673-2675 (1977).
11. R. M. Measures, "LIDAR Equation Analysis - Allowing for Target Lifetime, Laser Pulse Duration and Detector Integration Period", Appl. Optics, Vol. 16, 1092-1103 (1977).

12. R. M. Measures, "Laser Induced Fluorescence and Environmental Sensing", Invited paper for Optical Society of America, Topical Meeting on "Applications of Laser Spectroscopy", Paper FB5-1, Anaheim, California, March 19-21, 1975.

13. R. M. Measures, J. Garlick, W. R. Houston, D. G. Stephenson, "Laser Induced Spectra Signatures of Relevance to Environmental Sensing", Can. J. of Remote Sensing, Vol. 1, 95-102, Nov. 1975.

14. R. M. Measures, "Physical Constraints Associated with the Development of an Electrochemiluminescent Laser", Applied Optics, Vol. 14, 909-916 (1975).

15. R. M. Measures, W. R. Houston, D. G. Stephenson, "Laser Induced Fluorescent Decay Spectra - A New Form of Environmental Signature", Optical Engineering, Nov-Dec. 1974, Vol. 13, 494-501.

16. R. M. Measures, W. R. Houston and D. G. Stephenson, "Analyzing Fluorescence Decay", Laser Focus, Nov. 1974, 49-52.

17. R. M. Measures, "Prospects for Developing a Laser Based on Electrochemiluminescence", Applied Optics, Vol. 13, 1121-1133, May 1974.

BOOKS

R. M. Measures, "Analytical Use of Lasers in Remote Sensing", Chapter 6 of Analytical Laser Spectroscopy (Ed. N. Omenetto), J. Wiley Publications, 1979.

PROFESSIONAL PERSONNEL

Principal Investigator:

Dr. R. M. Measures (Professor of Applied Science and Engineering)

Research Assistants:

P. G. Cardinal (Commenced Ph.D.) - M.A.Sc. Thesis title, "The Importance of Seed Electron Creation and Single Photon Ionization to Laser Interactions Based on Resonance Saturation".

P. L. Wizinowich (Completing M.A.Sc.) - Thesis title, "Plasma Heating Based on Superelastic Laser Energy Conversion".

H. S. Kwong (Completed Ph.D.) - Thesis title, "Laser Ablation and Selective Excitation Directed to Trace Element Analysis".

M. R. Arnfield (Completing M.A.Sc.) - Thesis title, "Ion to Neutral Density Measurements in an Ablation Plasma Using Laser Selective Excitation Spectroscopy".

INTERACTIONS (COUPLING ACTIVITY)

Dr. R. M. Measures was invited to present a Seminar entitled, "Laser Selective Excitation Work at UTIAS" to the Physics Department of Toronto University on March 27, 1979.

In the past year Dr. R. M. Measures has had several discussions with Dr. J. Olsen of the Sandia Laboratory, in connection with the applicability of LIBORS to plasma channel formation for charged particle transportation in inertial confinement fusion. We are planning to discuss our recent work on "rapid plasma heating via superelastic laser energy conversion" with the group interested in X-ray laser development at the University of Rochester's Laboratory for Laser Energetics.

NEW DISCOVERIES STEMMING FROM RESEARCH

The combination of laser ablation and selective excitation spectroscopy (LASES) represents a new approach at evaluating fundamental atomic quantities, such as: radiative lifetimes, branching ratios, transition probabilities and selected collision cross-sections. A preliminary paper on this subject was published in Physical Review in 1977; see publication No. 9. The LASES technique, as well as being convenient and accurate, is particularly well suited for measurements on short lived, highly ionized species created by laser ablation and of interest in the development of X-ray lasers. Furthermore, the LASES approach is versatile and can use multiphoton or stepwise excitation as the means of generating the bursts of intensified emission.

As a spin-off of this work we have also shown that the LASES concept can also form the basis of a new form of trace element laser microprobe called a TABLASER; see publication No. 5.

During the past year we have reinforced our belief that "laser interaction based on resonance saturation", LIBORS, represents an ideal method of creating the plasma channels required for electron or ion beam transportation for inertial confinement fusion; see publication No. 2. We have also shown that under certain conditions LIBORS should have several advantages over inverse bremsstrahlung for plasma heating; see publication No. 3. In particular we have indicated that heating rates in excess of 10^{13} °K sec^{-1} would be achieved at relatively modest values of laser irradiance; see publication No. 1

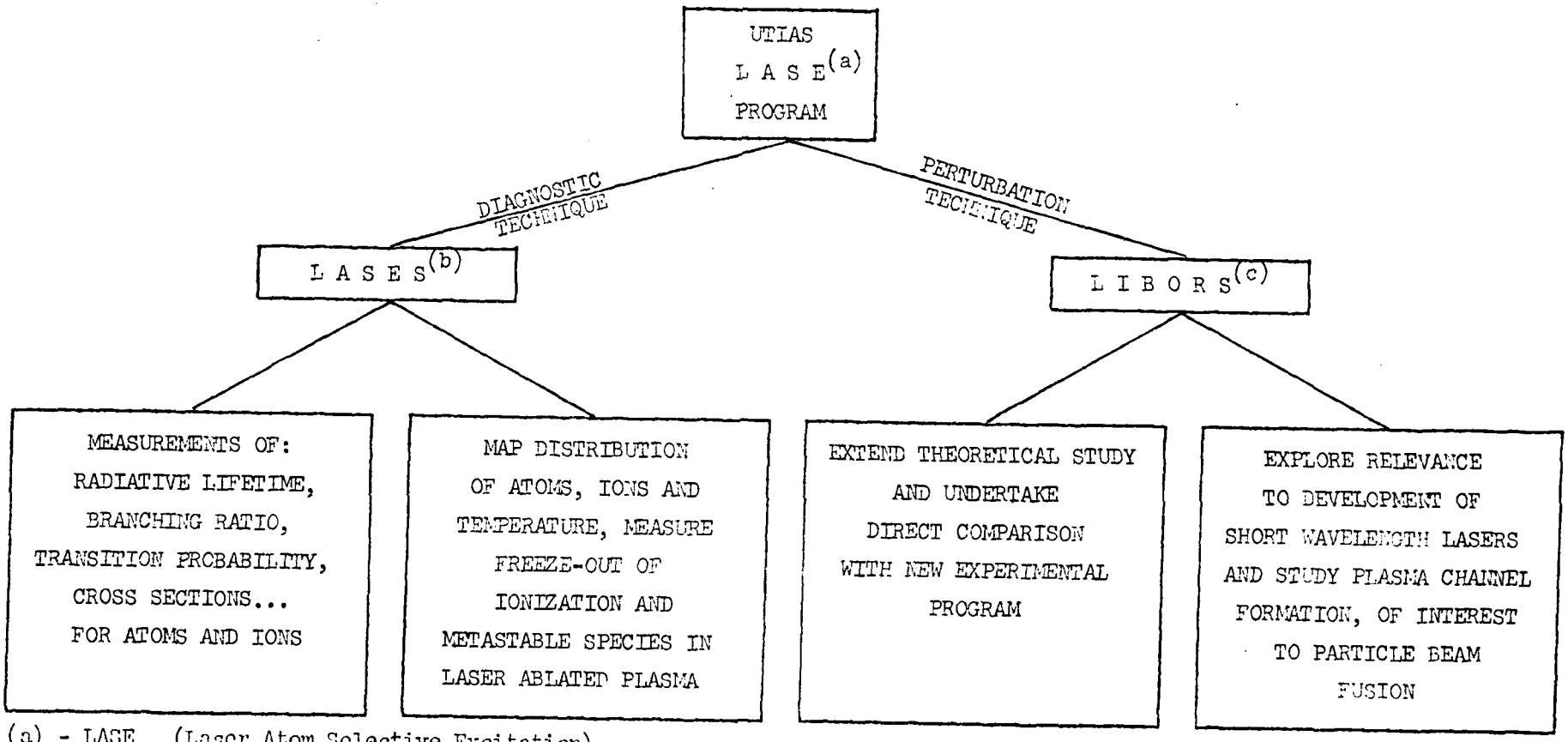

(a) - LASE (Laser Atom Selective Excitation)
(b) - LASES (Laser Ablation and Selective Excitation Spectroscopy)
(c) - LIBORS (Laser Interaction Based On Resonance Saturation)

FIGURE 1

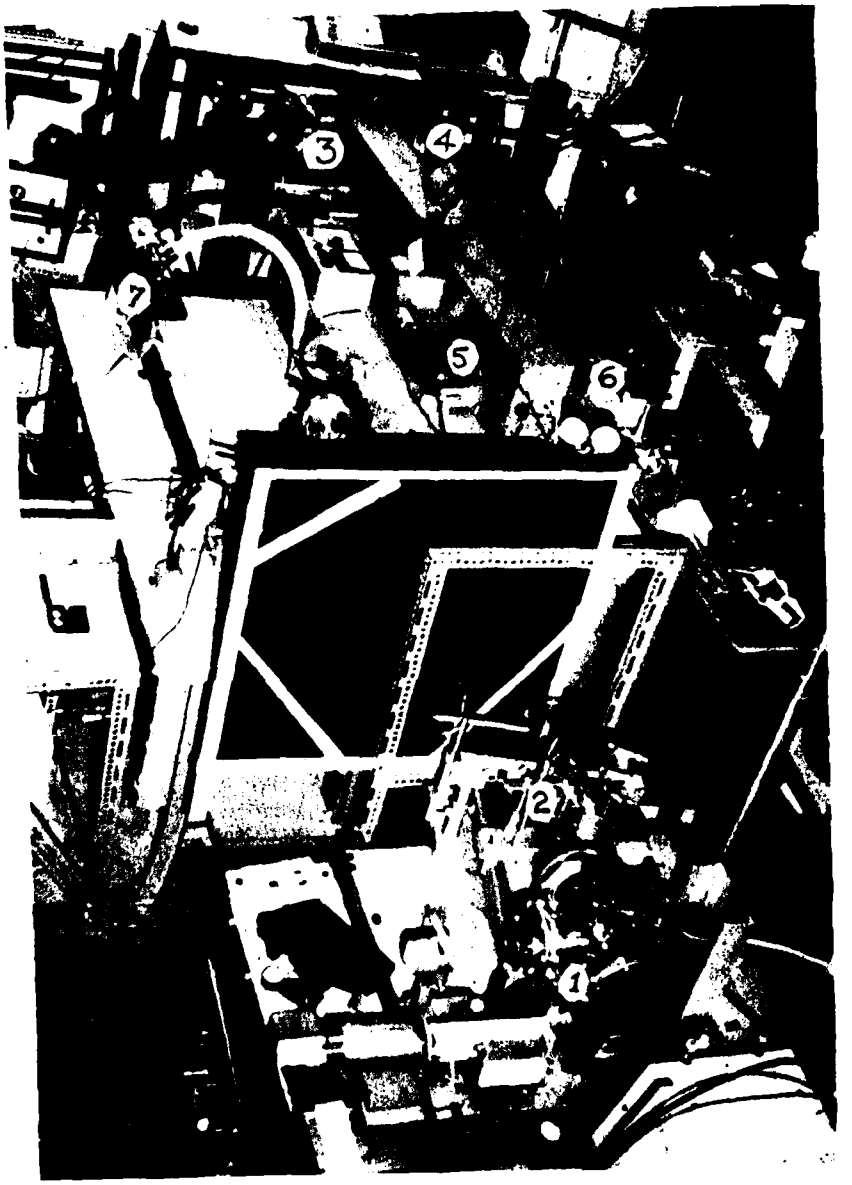

FIG. 2 Overview of LASES facility.

(1)	Ablation chamber and photodetection system
(2)	Dye laser input optics
(3) & (4)	Dye lasers
(5)	Nitrogen laser
(6)	Fabry-Perot system for checking dye laser wavelength
(7)	Q-switched Ruby (ablation) laser

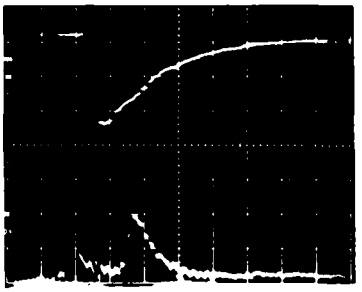

FIG. 3 Laser intensified spontaneous emission signals arising from an ablation plasma (1.2 μsec after ablation). The upper trace corresponds to the ISE signal from strontium atoms (at 460.7 nm) while the lower trace corresponds to the ISE signal from strontium ions (at 421.6 nm). The first pulse on the lower trace arises from a photodiode that monitors one of the dye lasers. Time scales are 20 nsec/div.

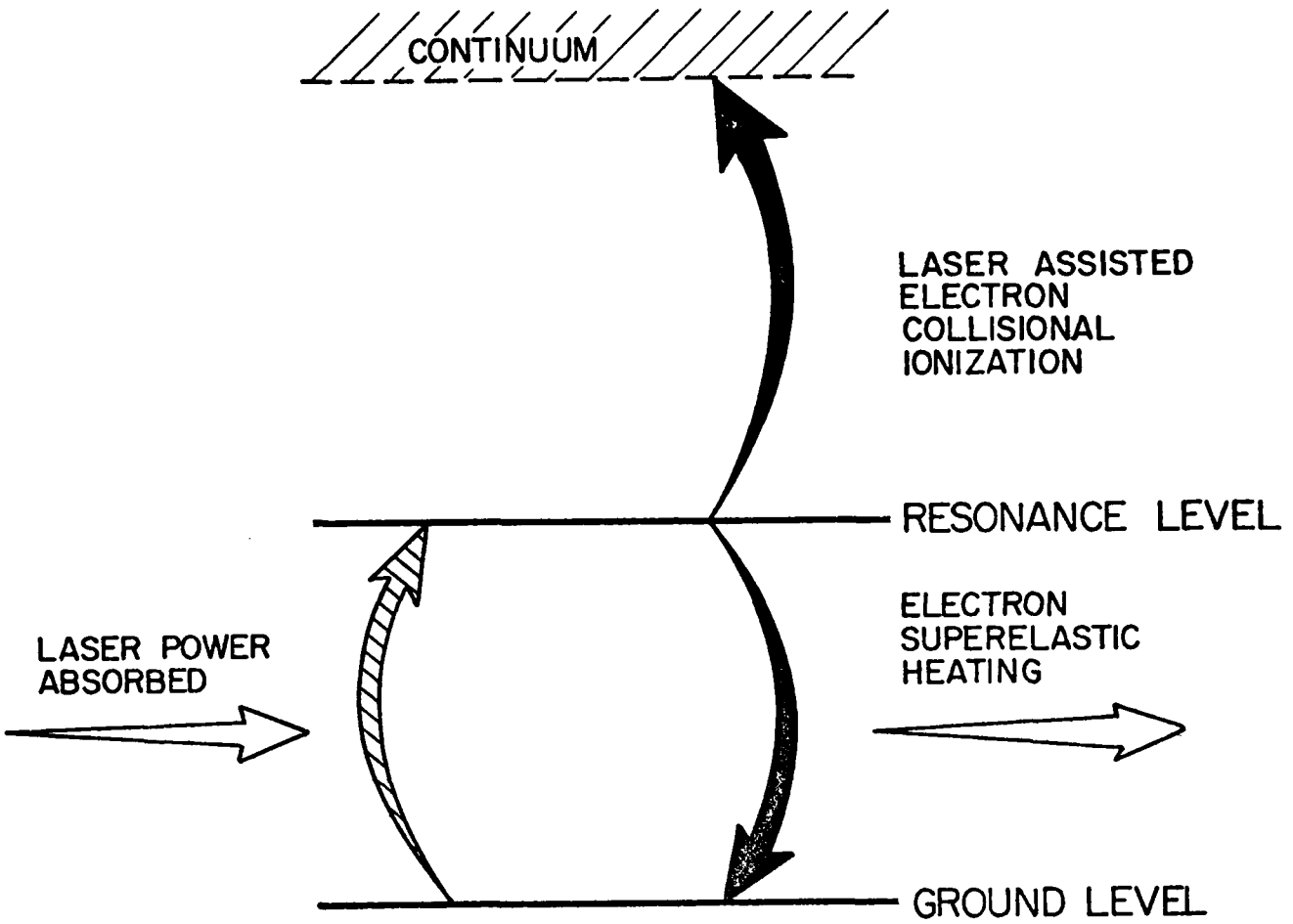

BASIC LIBORS PROCESSES

FIG. 4

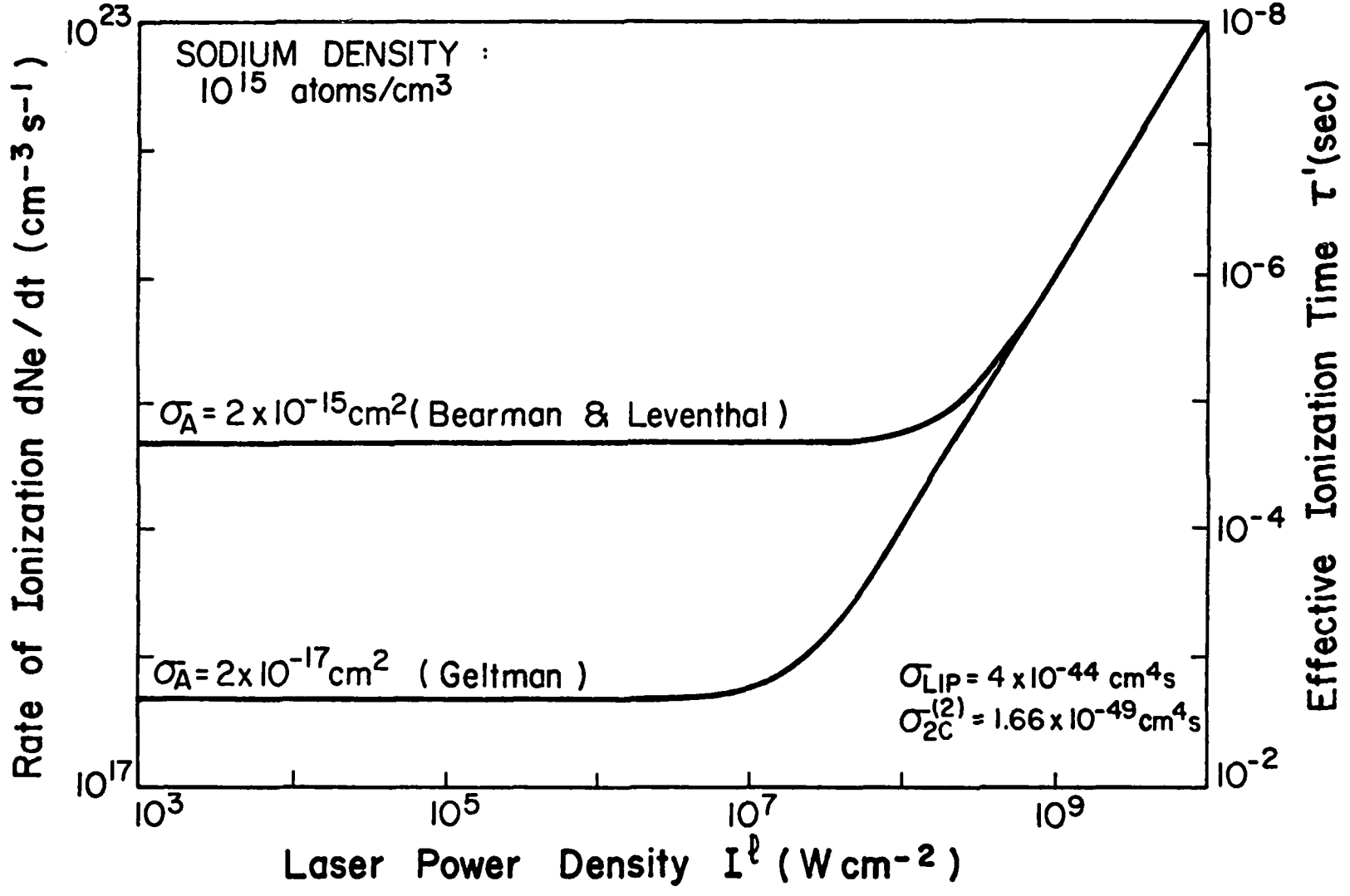

Fig. 5 dNe / dt vs I^{ℓ}

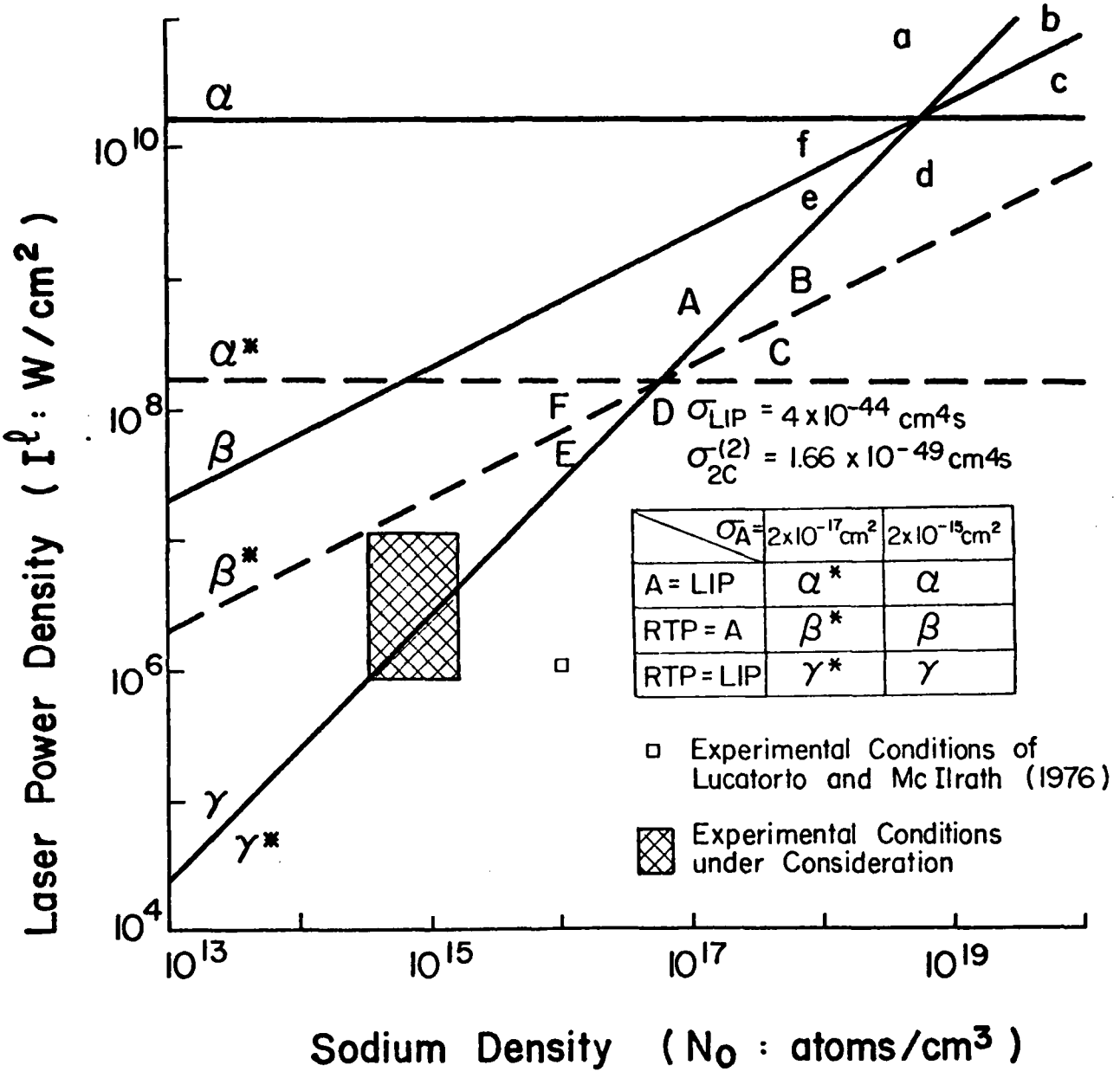

σ_A =	2×10^{-17}cm^2	2×10^{-15}cm^2
A = LIP	α*	α
RTP = A	β*	β
RTP = LIP	γ*	γ

Fig. 6 RELATIONSHIPS BETWEEN THE THREE SEED ELECTRON PROCESSES

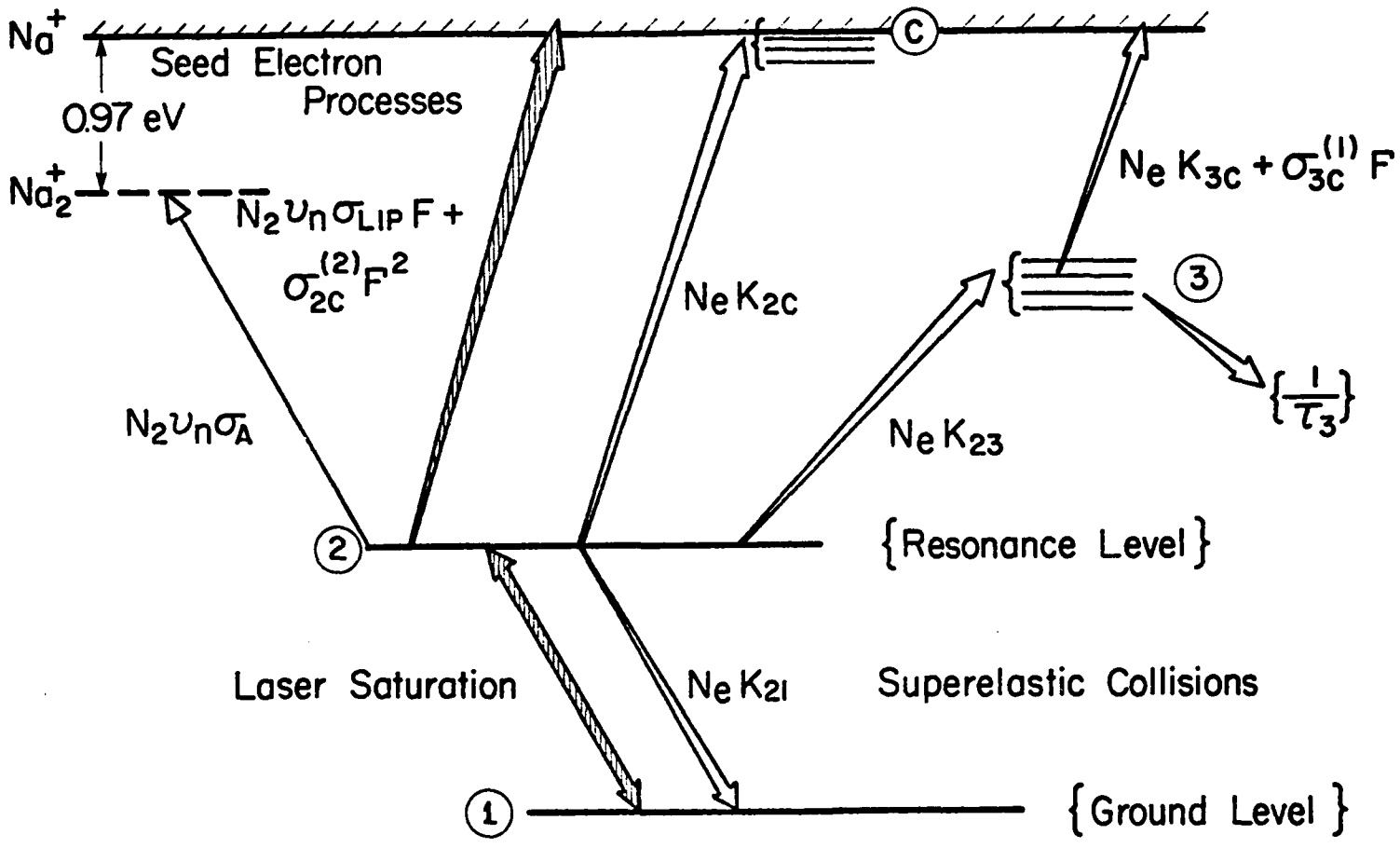

Fig. 7 SIMPLE MODEL OF LASER INTERACTION BASED ON RESONANCE SATURATION

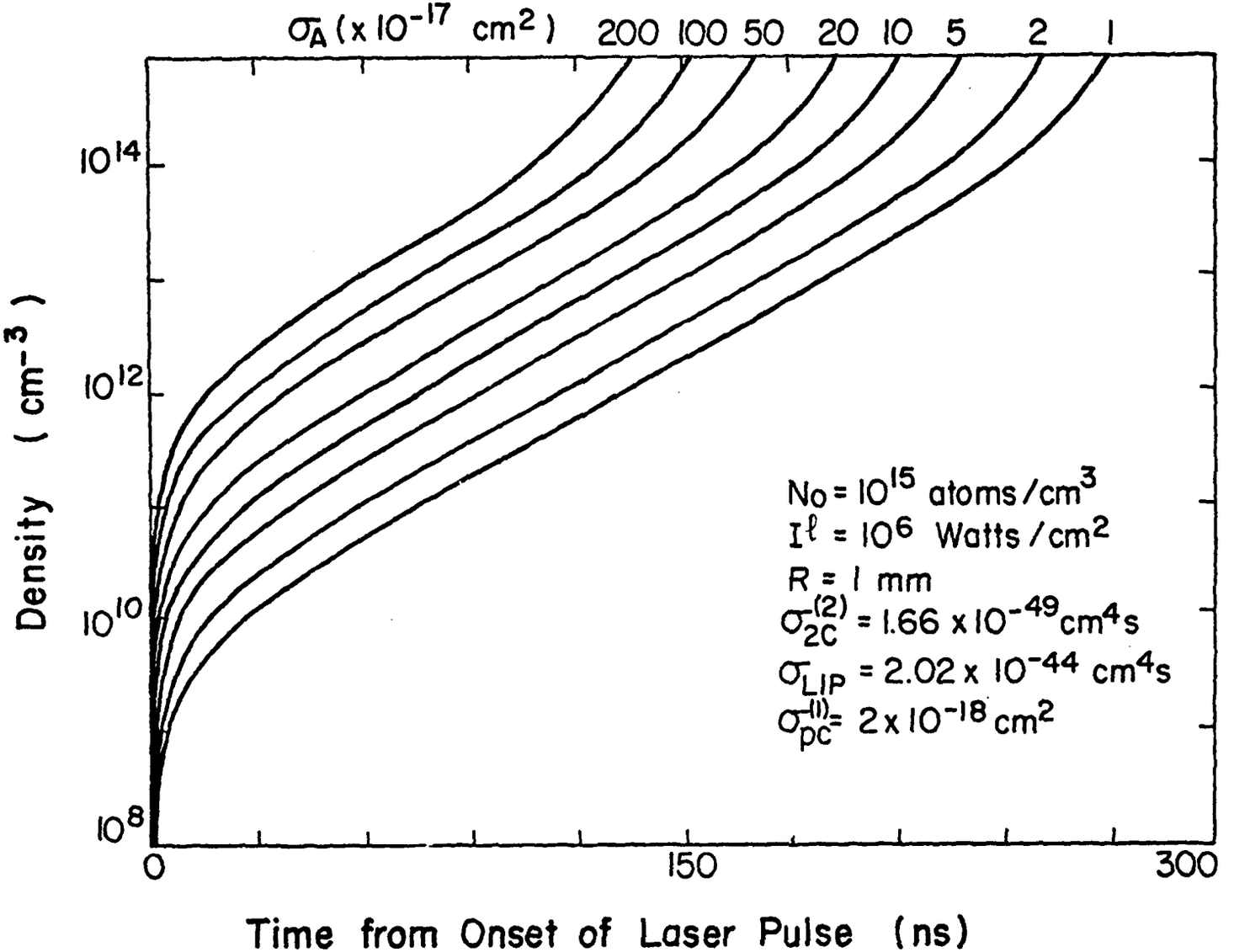

Fig. 8 EFFECT OF σ_A ON THE IONIZATION TIME

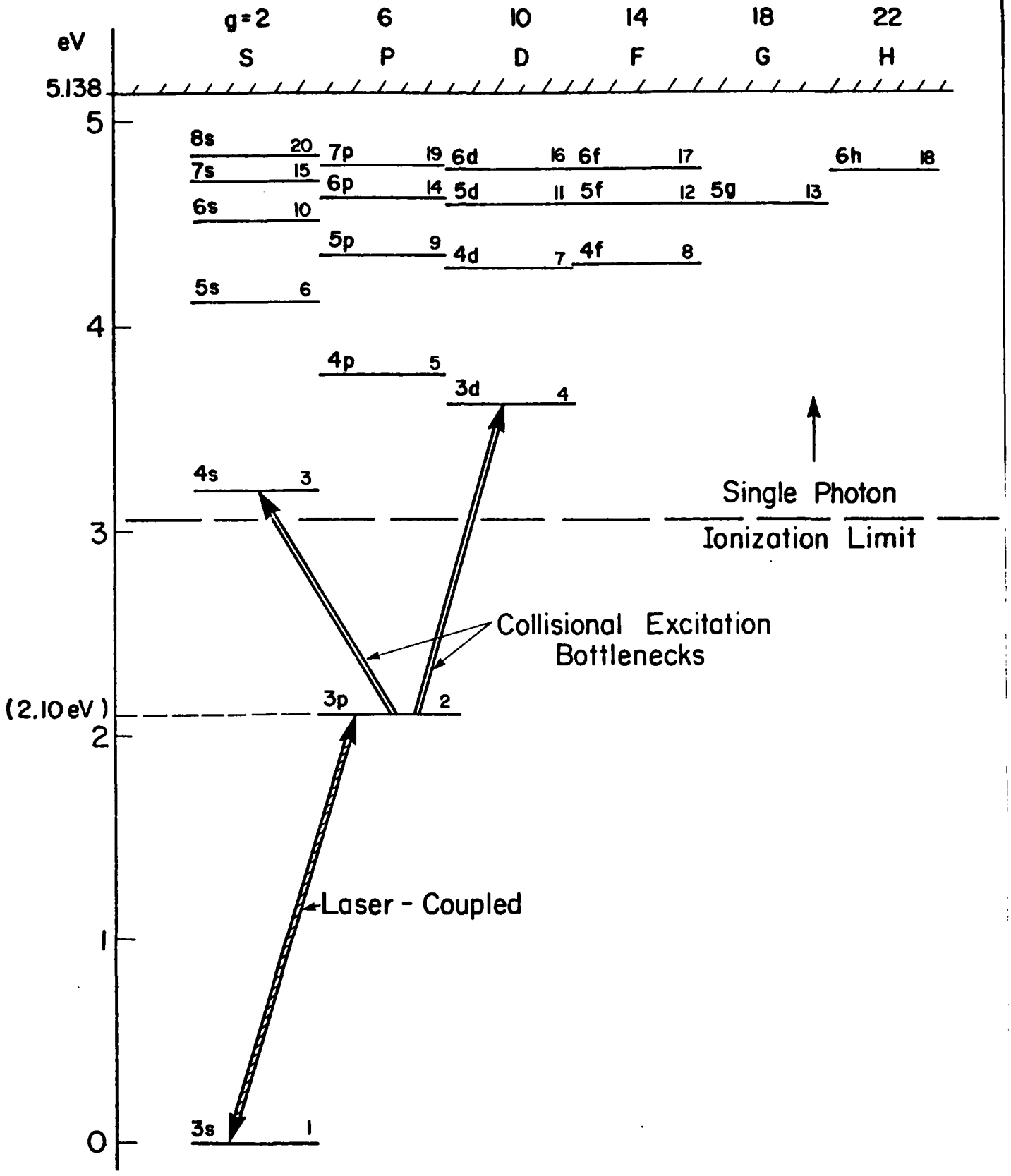

Fig. 3 Na: ENERGY LEVELS SCHEME USED IN LIBORS PROGRAM

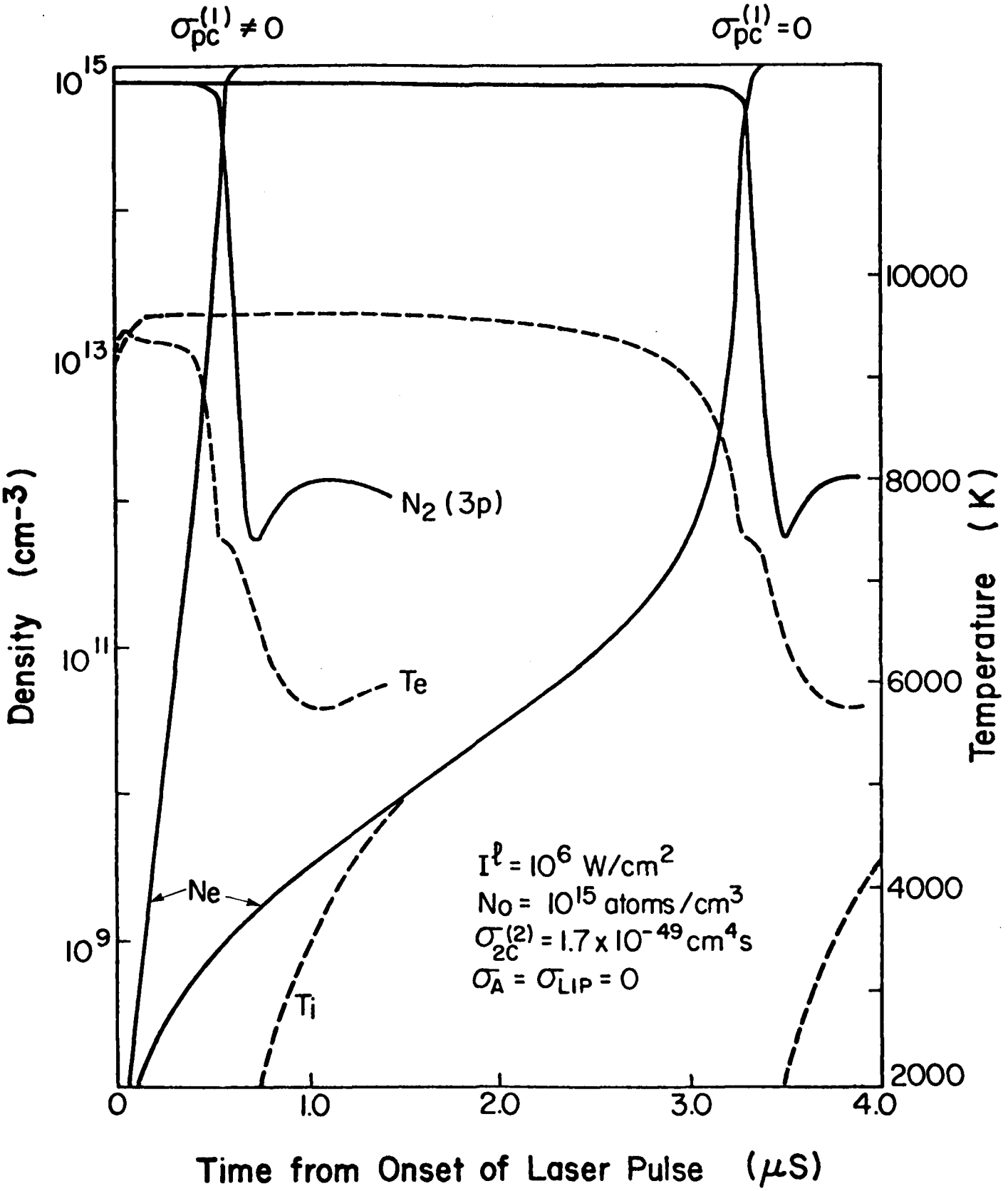

Fig. 10 COMPARISON OF LIBORS COMPUTER RESULTS WITH AND WITHOUT SINGLE PHOTON IONIZATION

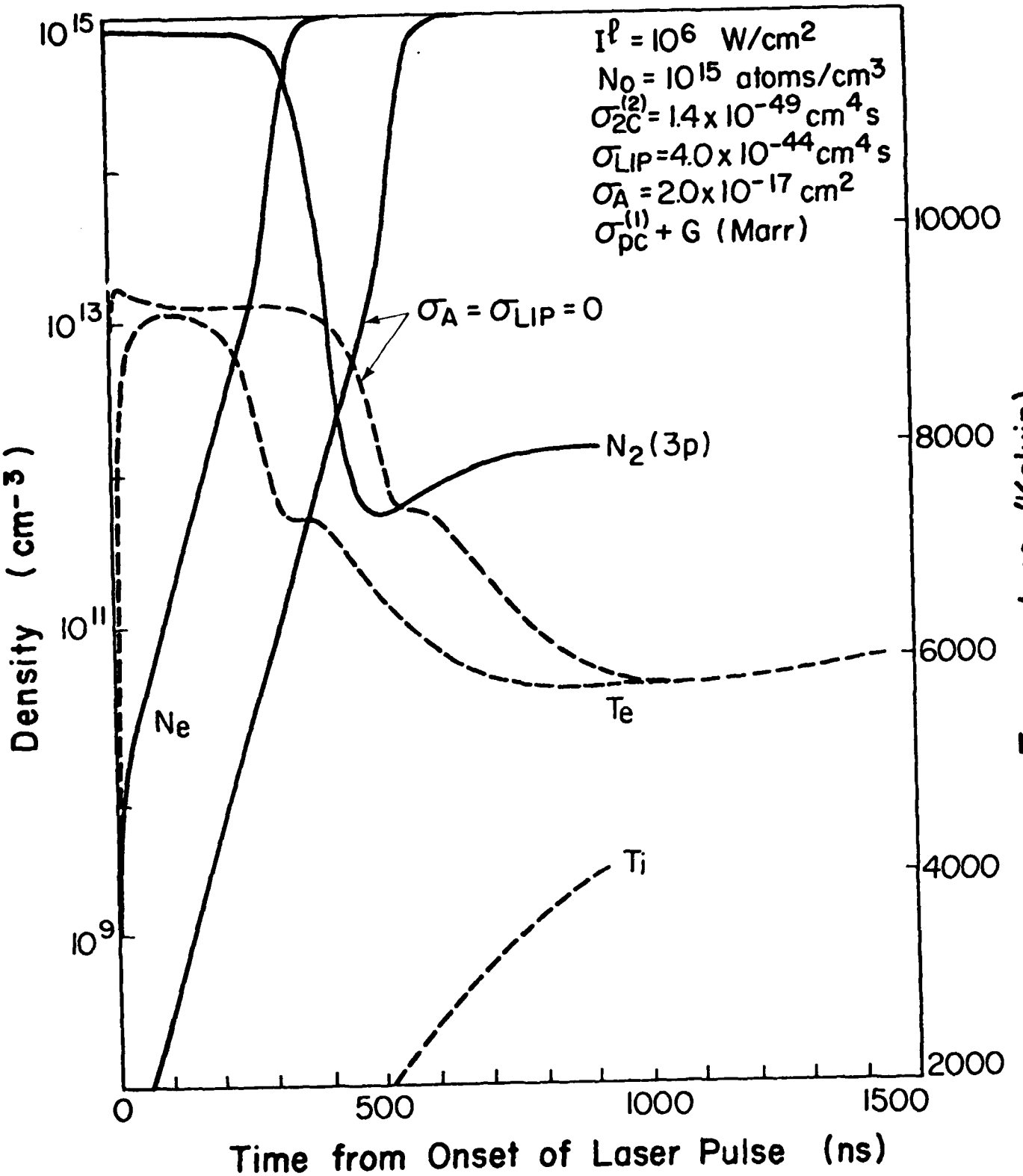

Fig. TEMPORAL BEHAVIOUR OF N_2, Ne, Te AND Ti WHEN ALL SEED ELECTRON PROCESSES ARE INCLUDED

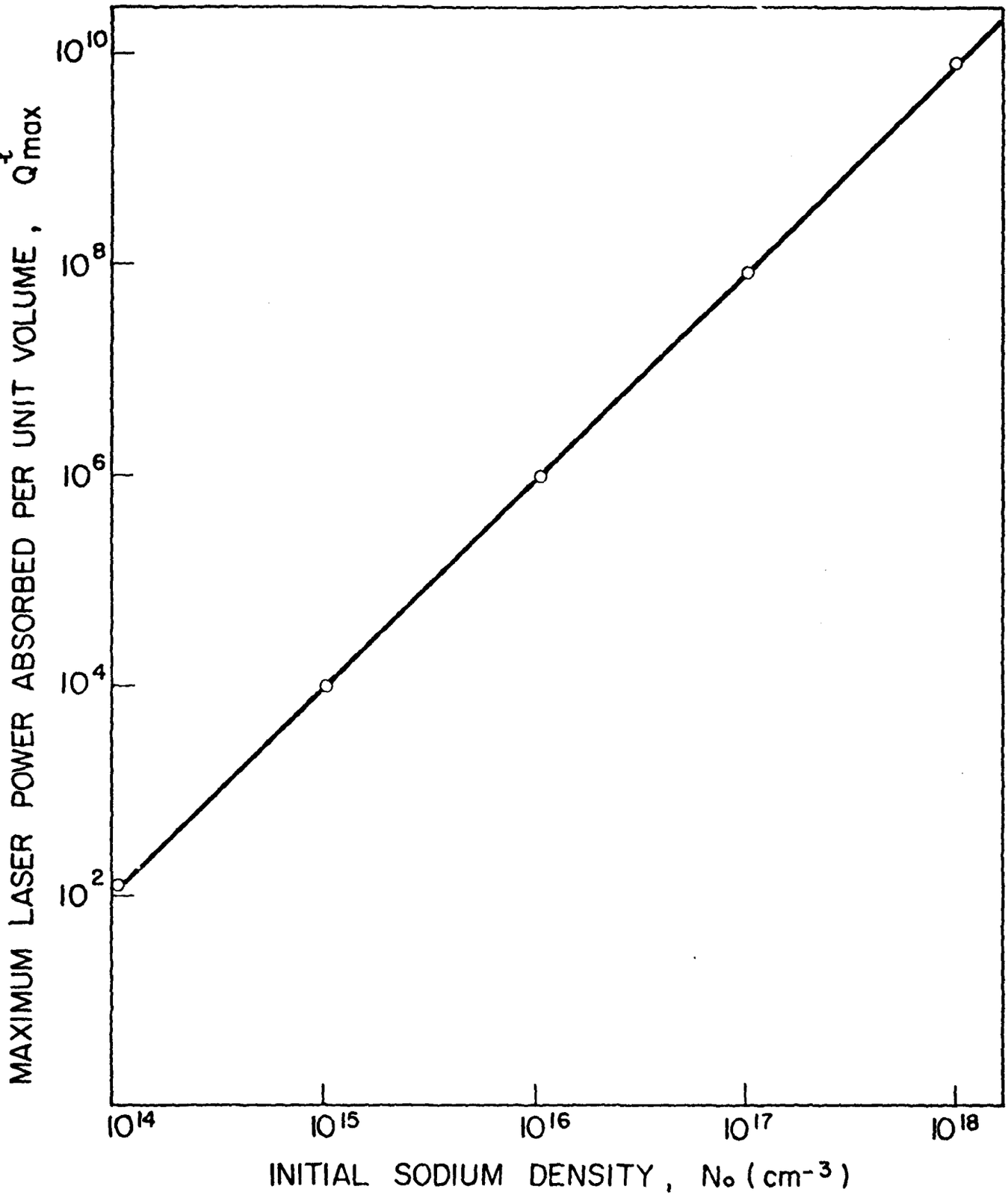
MAXIMUM LASER POWER ABSORBED PER UNIT VOLUME, Q^{ℓ}_{max}
10^{10}
10^{8}
10^{6}
10^{4}
10^{2}
10^{14}
10^{15}
10^{16}
10^{17}
10^{18}
INITIAL SODIUM DENSITY, N_o (cm^{-3})

FIG. 12

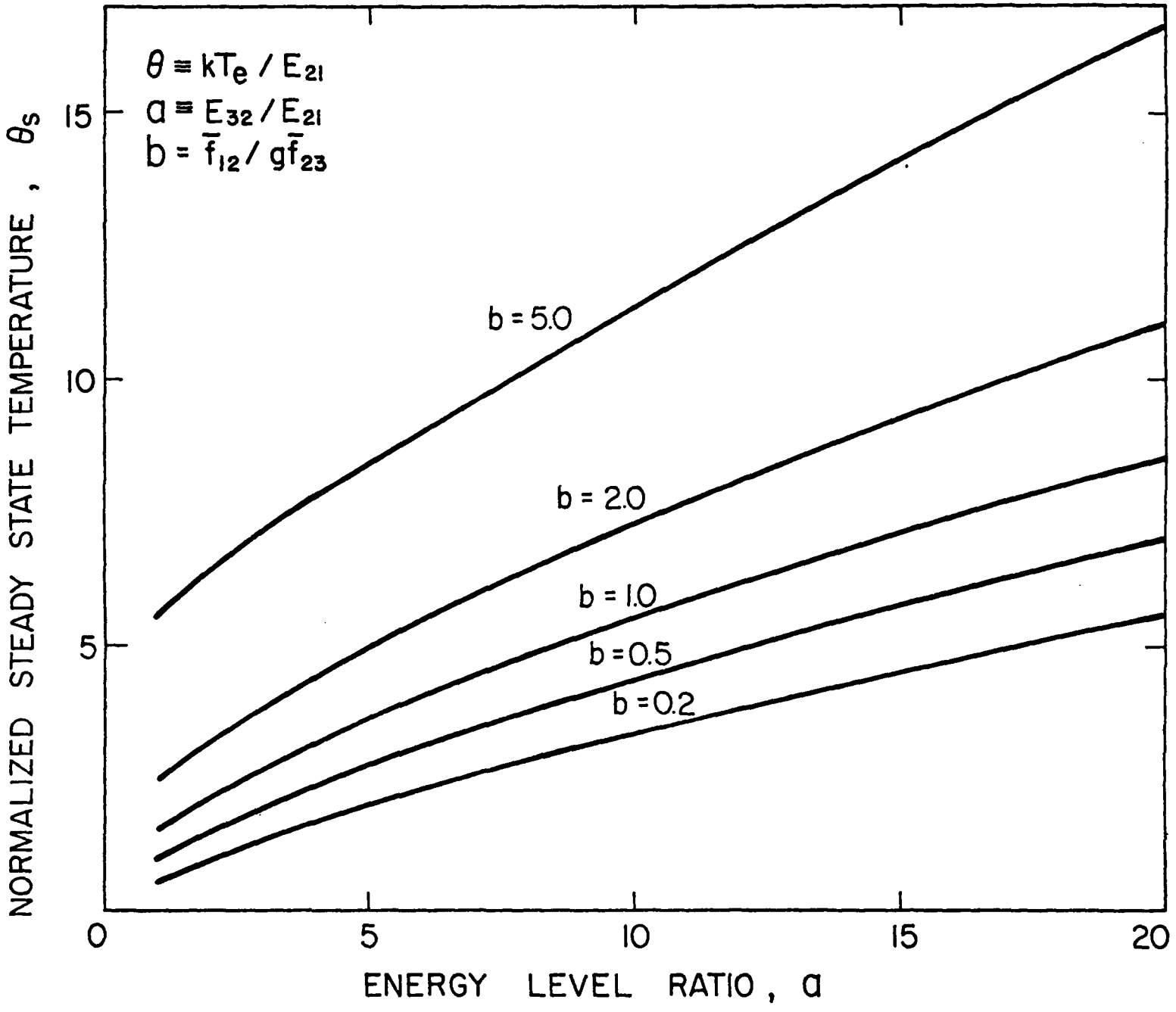
θ ≡ kTe / E21
a ≡ E32 / E21
b = f̄12 / gf̄23
b = 5.0
b = 2.0
b = 1.0
b = 0.5
b = 0.2
NORMALIZED STEADY STATE TEMPERATURE , θs
ENERGY LEVEL RATIO , a
0
5
10
15
20

FIG 13

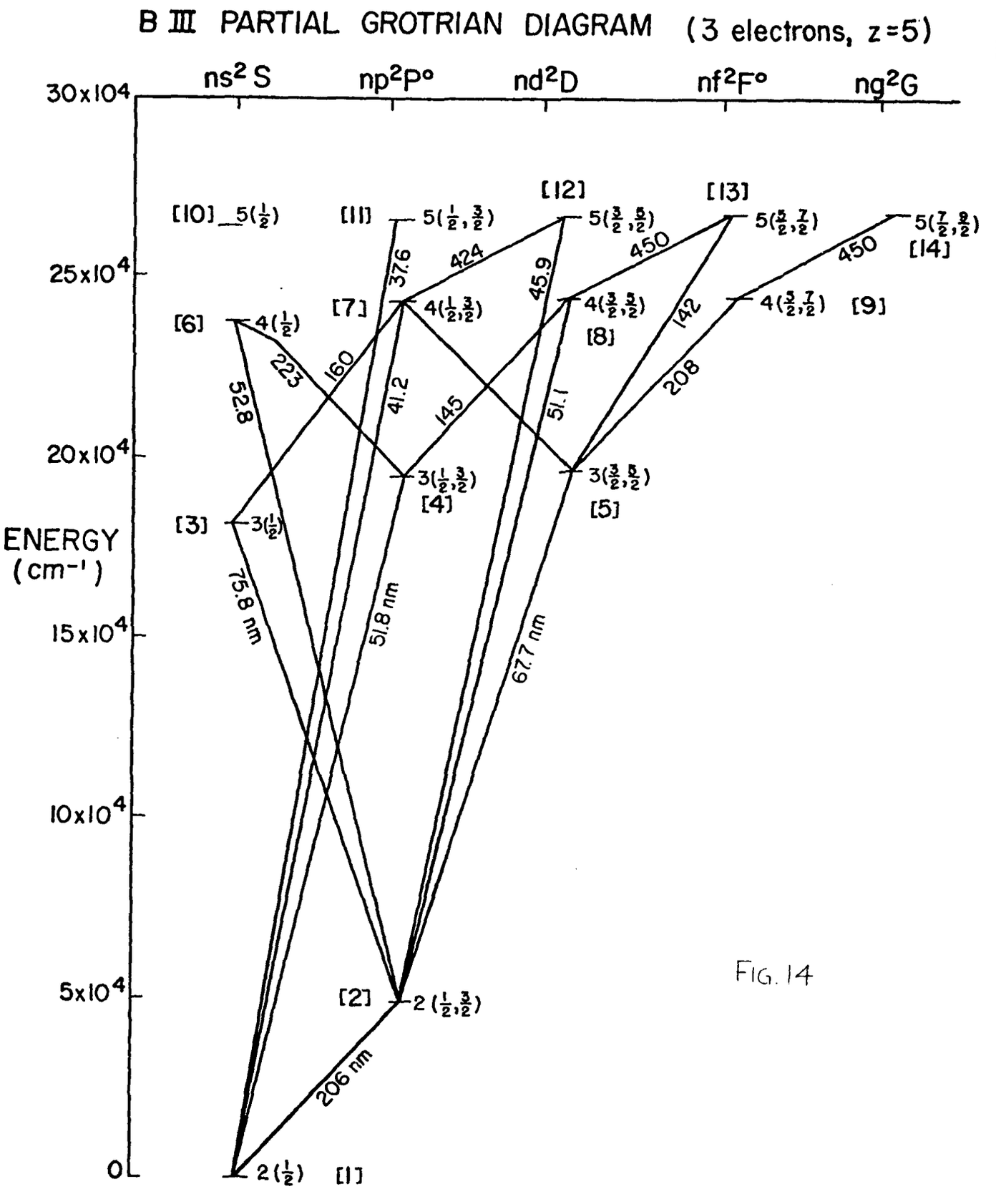
B III PARTIAL GROTRIAN DIAGRAM (3 electrons, z=5)
ns² S
np² P°
nd² D
nf² F°
ng² G
30x10⁴
25x10⁴
20x10⁴
15x10⁴
10x10⁴
5x10⁴
0
ENERGY (cm⁻¹)
[10] 5(½)
[11] 5(½,3/2)
[12]
[13]
5(3/2,5/2)
5(5/2,7/2)
5(7/2,9/2)
[14]
[6] 4(½)
[7] 4(½,3/2)
4(3/2,5/2)
[8]
4(5/2,7/2)
[9]
[3] 3(½)
3(½,3/2)
[4]
3(3/2,5/2)
[5]
[2] 2(½,3/2)
2(½)
[1]
37.6
424
45.9
450
450
142
223
160
145
208
52.8
41.2
51.1
75.8 nm
51.8 nm
67.7 nm
206 nm

FIG. 14

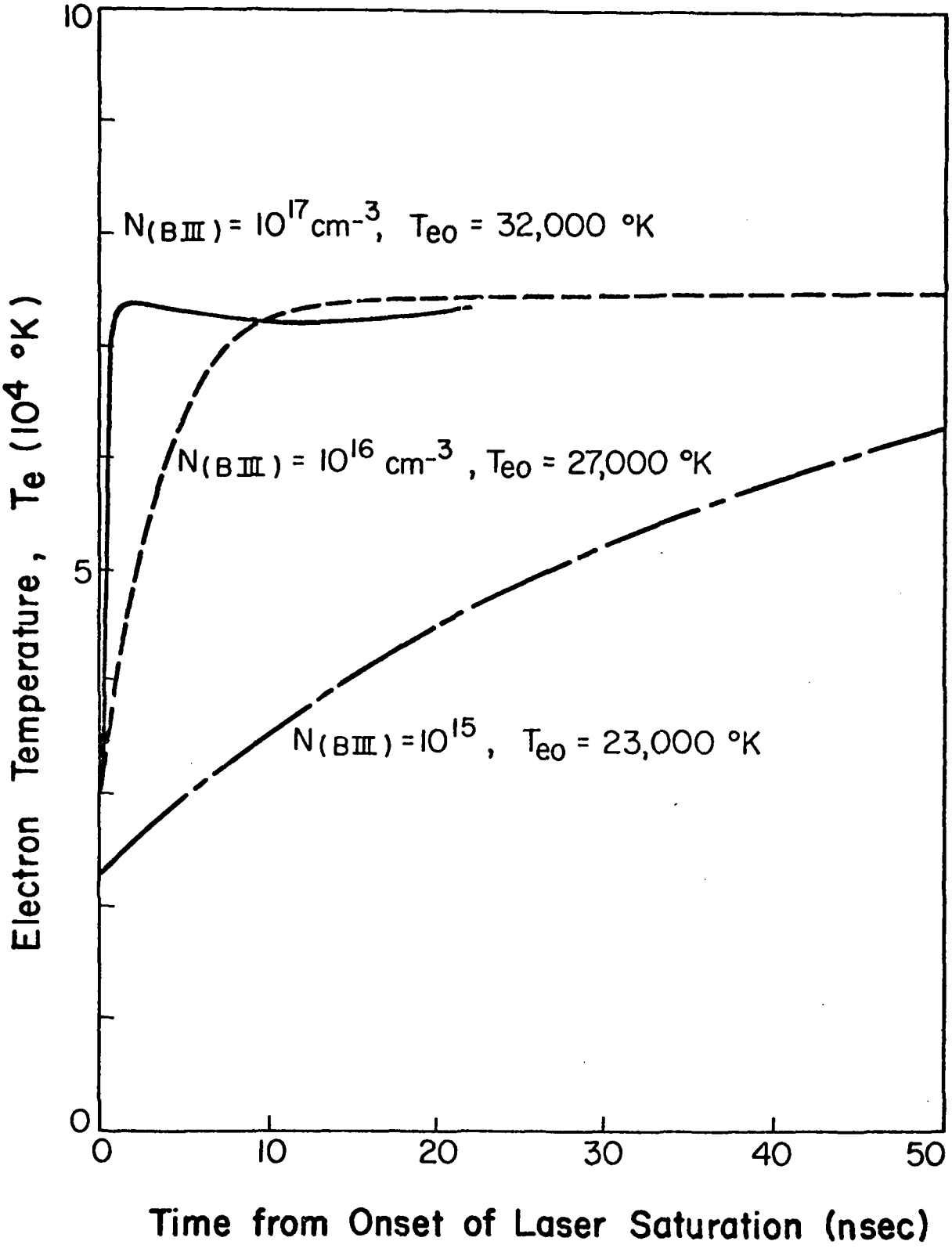
10
5
0
0
10
20
30
40
50
N(B III) = 10^17 cm^-3, Teo = 32,000 °K
N(B III) = 10^16 cm^-3, Teo = 27,000 °K
N(B III) = 10^15, Teo = 23,000 °K
Electron Temperature, Te (10^4 °K)
Time from Onset of Laser Saturation (nsec)

FIG. 15

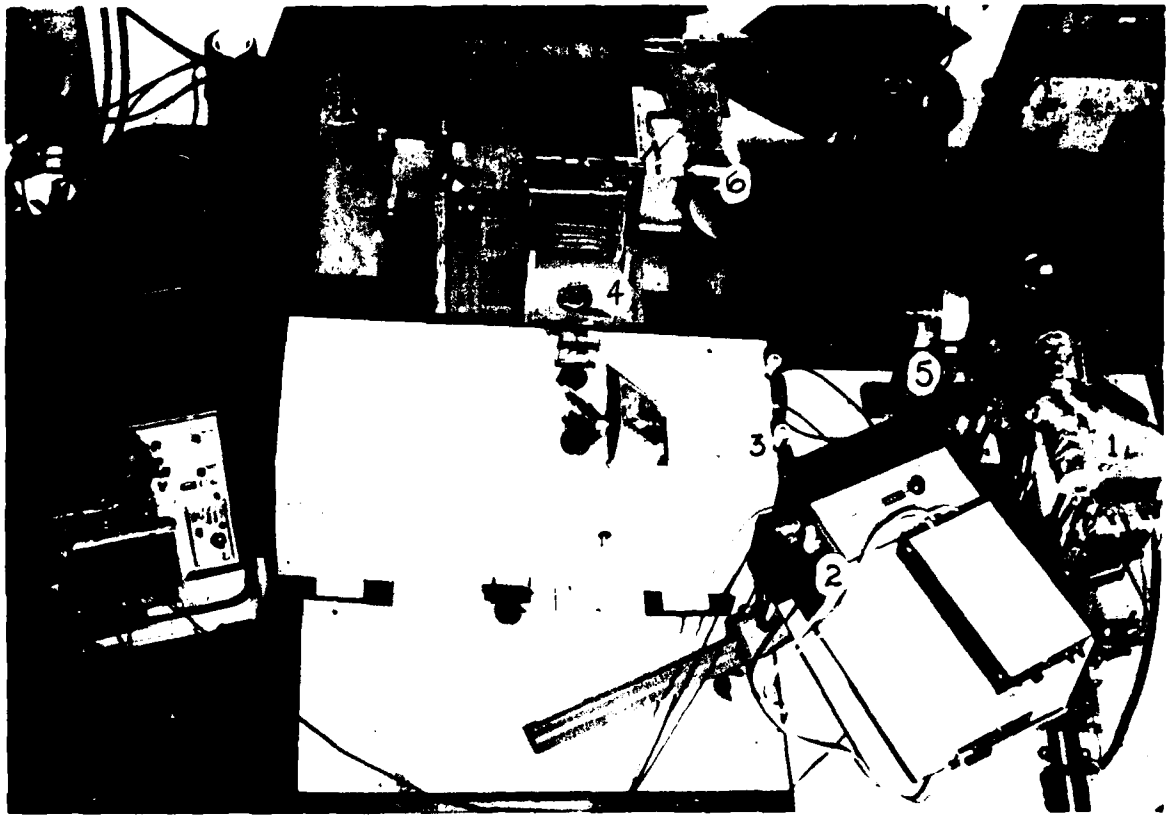

FIG. 16 An overview of the preliminary LIBORS facility.

(1) Sodium vapour cell
(2) IP21-PME and Heath Monochromator
(3) SPEX Monochromator (used as spectrograph)
(4) Camera-C2
(5) Laser transmission photodiode-PD
(6) Camera-C1

Fig. 17 LIBORS FACILITY

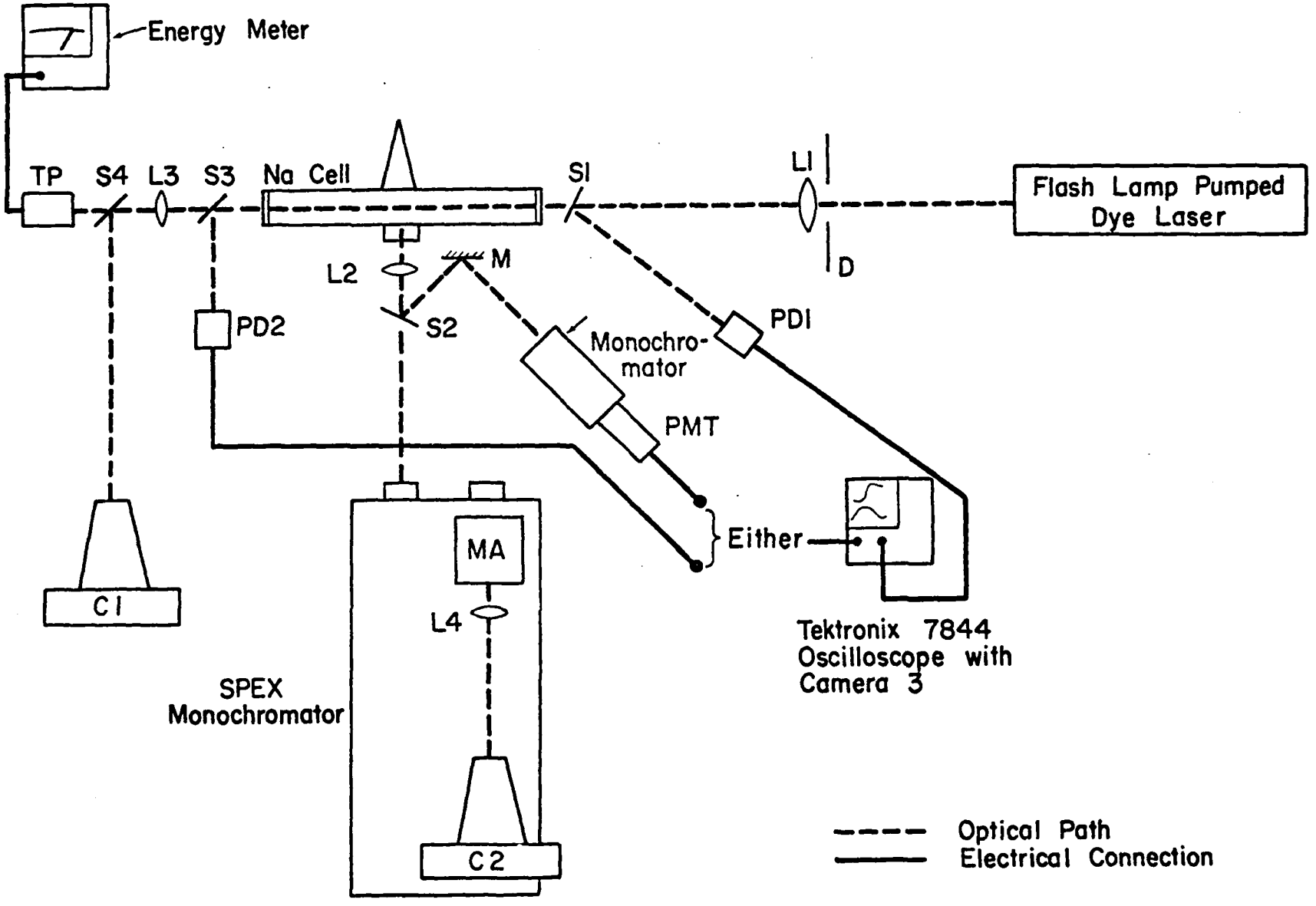

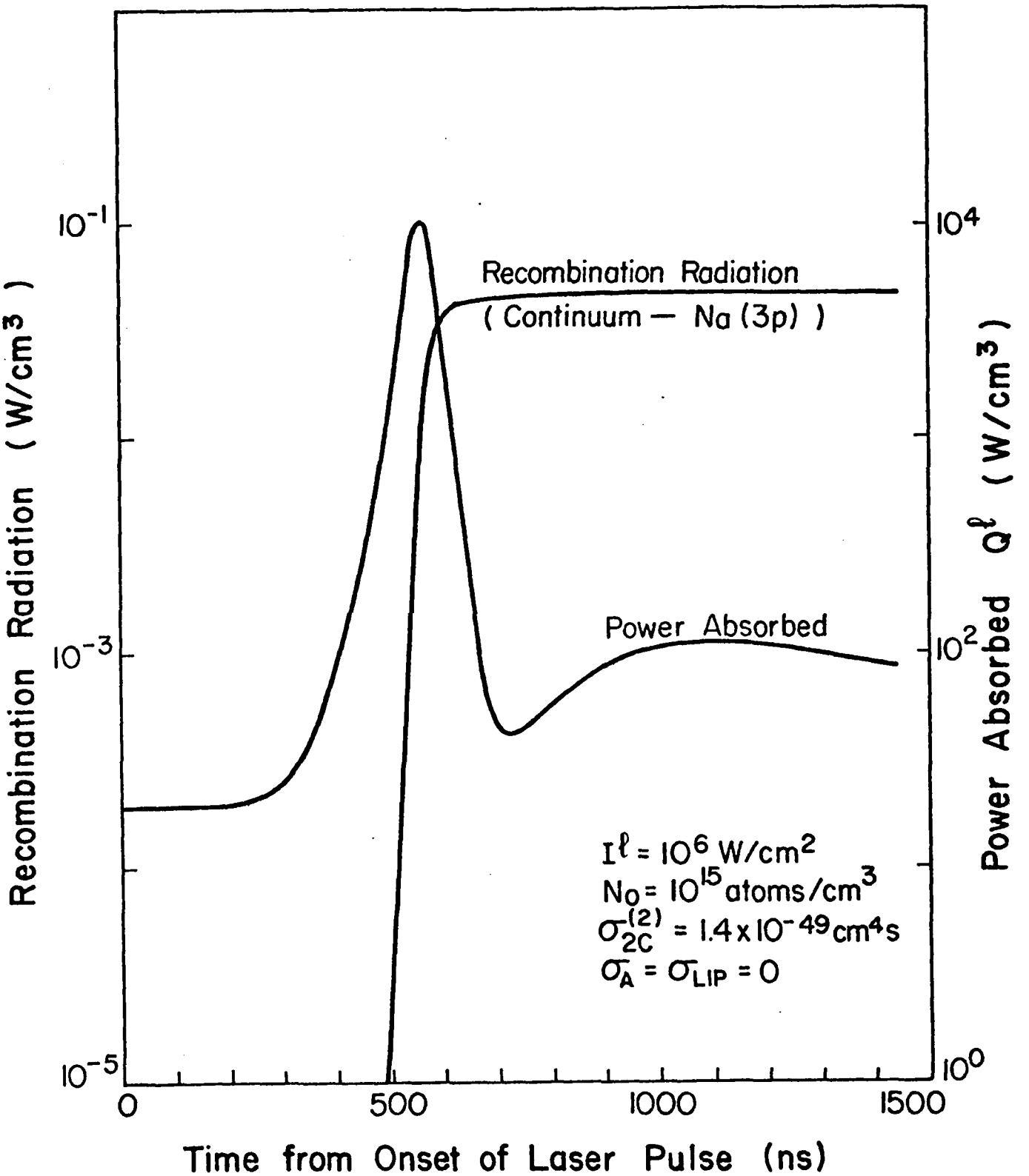

Fig. 18 POWER ABSORBED BY VAPOUR AND RECOMBINATION TO THE Na (3p) STATE

APPENDIX A

REVIEW OF LASER SELECTIVE EXCITATION SPECTROSCOPY

The concept of laser selective excitation spectroscopy was first formulated by the author,[1] and one of the first tests of the technique was undertaken in this laboratory.[2] Subsequently, the ideas embodied in this paper have found wide application in fields ranging from flame studies[3] to fusion reactor diagnostics.[4] We have demonstrated that the combination of laser ablation and selective excitation spectroscopy represents an ideal method of determining atomic parameters such as radiative lifetimes, branching ratios and transition probabilities of elements that are difficult to handle[5] and are planning to show that this approach can be extended to include excited states of ions. Currently we are attempting to evaluate the potential of selective excitation spectroscopy in the context of undertaking a direct measurement of the degree of ionization of a specific constituent within a rapidly expanding plasma.

In particular, we are using two nitrogen laser pumped dye lasers to pump two resonance transitions; one in neutral strontium and the other in singly ionized strontium (at 460.7 and 421.6 nm, respectively). The plasma is produced by laser ablation of a strontium doped target. Initially we plan to study the variation (at a given location) in the degree of ionization as a function of elapsed time from the moment of ablation.

The theoretical development presented below is based on the treatment provided in UTIAS Report No. 229 (1979) by N. Drewell. We shall consider the population redistribution that results when two energy levels of an atom (or an ion) are suddenly coupled by a step-like pulse of laser radiation. The population rate equation treatment presented is valid provided the laser radiation is broad band (relative to the linewidth of the excited transition) and the dephasing collision time is shorter than times of interest.[6]

The rate equations for levels j and i can be expressed in the form

$$\dot{N}_j = N_i(R_{ij} + N_e K_{ij}) - N_j(R_{ji} + A_{ji} + N_e K_{ji} + D_j) + C_j \qquad (1)$$

$$\dot{N}_i = N_j(R_{ji} + N_e K_{ji} + A_{ji}) - N_i(R_{ij} + N_e K_{ij} + D_i) + C_i \qquad (2)$$

where $\dot{N}_i$ and $\dot{N}_j$ are the time derivatives of N_i and N_j, respectively. Figure A1 shows schematically the two laser-coupled energy levels i and j with expressions for the rates (per unit volume) of the various processes under consideration. Also, the rate coefficients D_i and D_j have been used to represent all processes which deplete levels i and j respectively, exclusive of those that couple the two levels. In a similar manner C_i and C_j have been employed to represent the rates of populating levels i and j respectively, exclusive of the interactions that directly couple levels i and j.

Introducing time-invariant rates (the C's) and rate coefficients (the D's) in this way simplifies the problem because only the populations N_i and N_j need be considered explicitly. As a result, however, the validity of the solution of these equations is restricted to times shorter than that required to appreciably alter the populations in the other levels of the atom and the electron density, because the C's and D's are functions of these variables. In a similar fashion, writing K_{ij} and K_{ji} as time invariant implies that we are assuming a constant electron temperature throughout the analysis (the C's and D's are in general also electron temperature dependent), and similarly restricts the validity of the solution. These points were not raised by Burgess and Skinner[7] who presented a simplified analysis of the same problem. Indeed, as was first pointed out by the author[8] dramatic changes in both the free electron density and temperature occur if laser pumping is continued for an extended period of time.

The above coupled set of differential equations can be decoupled to form two second order differential equations. The equation for N_j takes the form

$$\ddot{N}_j + A\dot{N}_j + BN_j = C \qquad (3)$$

where

$$A = N_e(K_{ij} + K_{ji}) + A_{ji} + D_i + D_j + R_{ij} + R_{ji} \qquad (4a)$$

$$B = D_i(R_{ji} + D_j + A_{ji} + N_e K_{ji}) + D_j(R_{ij} + N_e K_{ij}) \qquad (4b)$$

$$C = C_i(R_{ij} + N_e K_{ij}) + C_j(R_{ij} + N_e K_{ij} + D_i) \qquad (4c)$$

The solution to Eq. (3) can be expressed in the form

$$N_j(t) = C/B + E_1 e^{\lambda_1 t} + E_2 e^{\lambda_2 t} \tag{5}$$

where

$$\lambda_{1,2} = -A/2 \pm \frac{A}{2}\left(1 - \frac{4B}{A^2}\right)^{\frac{1}{2}} \tag{6}$$

The form of the solution depends on the particular values of C_i, C_j, D_i, D_j and on the initial conditions. In order to show qualitatively the variety of possible forms of solution we set $N_i(0) = N_o$ and $N_j(0) = sN_o$ where N_o is the population of the lower level, and s is a free parameter which represents the ratio of N_j/N_i, evaluated prior to laser coupling. Under these initial conditions we obtain

$$E_2 = sN_o - C/B - E_1 \tag{7}$$

and

$$E_1 = N_o(R_{ij} - sR_{ji}) + \lambda_2(C/B - sN_o)/(\lambda_1 - \lambda_2) \tag{8}$$

We assign a value to D_i and define a free parameter Q such that $Q = D_j/D_i$. C_i and C_j could similarly be assigned certain values, however, we use C_i and C_j to impose the steady state condition on the system prior to laser coupling, i.e., we set $\dot{N}_j\ (t < 0) = \dot{N}_i\ (t < 0) = 0$ from which it follows that

$$C_i = N_o[D_i + N_e(K_{ij} - sK_{ji}) - sA_{ji}] \tag{9}$$

and

$$C_j = N_o[s(D_j + A_{ji}) + N_e(sK_{ji} - K_{ij})] \tag{10}$$

Note that

$$C_i + C_j = N_o(sD_j + D_i) \tag{11}$$

and since C_i and C_j are greater than zero by definition, (9) and (10) show that the values of the variables on the RHS's are not completely arbitrary.

The temporal forms of intensified spontaneous emission (ISE) from level j, for various values of the free parameters, are shown in Fig. A2 on the assumption that this emission is directly proportional to $A_{ji}N_j(t)$. The

laser-induced rate coefficients R_{ij} and R_{ji} were set equal to ten times the rate coefficient D_i, viz., in the computational work we have set the degeneracy ratio of i and j to be unity. The electron collision quenching probability $N_e K_{ji}$ and the spontaneous emission probability A_{ji} were both set equal to $D_i/10$. The time axis is in terms of D_i^{-1} and the vertical scale has been normalized by the j level population prior to laser saturation so that the spontaneous emission before laser turn-on equals unity. In Fig. A2 the step-function laser irradiation starts at t = 0, and the initial sharp change in spontaneous emission reflects the laser induced redistribution of the population between levels i and j.

Positive-going signals refer in general to cases where $N_j < N_i$ for $t \leq 0$, which apply to all cases of thermal plasma; curves A, B and C refer specifically to the case where $N_j = N_i/5$ for $t \leq 0$. Negative going signals refer in general to cases where $N_j > N_i$ for $t \leq 0$, which apply to all cases of "inverted" populations. These D, E and F curves (shown in Fig. A2) refer specifically to the case where $N_j = 5N_i$ for $t \leq 0$. The special case of $N_j = N_i$ is represented by curve G, which shows no deflection on laser turn-on.

The positive and negative deflections are further classified according to the ratio $Q = D_j/D_i$. For a given s, Q is a measure of the change in the rate of loss of population from the set of laser coupled levels due to the laser induced internal redistribution. For $Q > 1$ and $s < 1$ (e.g., curve C for $Q = 2$, $s = 0.2$ in Fig. A2), the spontaneous emission declines after the initial jump, because the pair of laser-coupled levels loses population faster (via $N_j D_j$ and $N_i D_i$) than can be supplied by the sum of rates $C_i + C_j$. This form of solution (curve C) has been analysed in detail by Measures[1] within the context of plasma diagnostics.

For $Q < 1$ and $s < 1$ (e.g., curve A for $Q = 0.5$, $s = 0.2$ in Fig. A2), the spontaneous emission continues to increase after the initial rise, achieving a steady state value somewhat greater than that for curve B. In this case the population loss rate via $N_j D_j + N_i D_i$ has been decreased by the laser induced redistribution of populations in levels i and j.

When $Q = 1$, $D_j = D_i$ and therefore no change in population loss rate via $N_j D_j + N_i D_i$ occurs due to the laser induced redistribution. Curves D, E, and F are the population inversion equivalents of curves C, B, and A respectively, and represent media which exhibit optical gain. In these cases the onset of laser action in a laser cavity or the penetration of a laser beam in a laser

amplifier will cause a sudden decrease in the spontaneous emission from the upper level (and an increase from the lower level if such transitions are allowed). This effect has been observed[9-11] during the course of investigations into lasing media.

The conditions that applied to curve C in Fig. A2 have been used to form a three dimensional plot of normalized ISE signals against time using the logarithm of the ratio of the laser-induced rate coefficient R_{ij} ($= R_{ji}$) to the loss coefficient D_i as the third dimension. Figure A3 illustrates the change in the temporal variation of the ISE with increasing laser coupling. R_{ij} varies in steps of $10^{1/2}$ D_i from $10^{-7/2}$ D_i at the front to 10^{4} D_i at the back. Note that at suitably high laser powers ($R_{ij} > 10\ D_i$), the shape of the ISE curve has only a weak dependence on R_{ij} - this in fact is what is implied by saturation.

Figure A4 shows the ISE curves for the special case of resonance pumping. In this graph we have assumed that $D_i = D_j = 0$, and therefore the time is given in units of A_{21}^{-1}. In addition, we have assumed that $N_2(0) = 0$ and therefore that $C_i = C_j = 0$. The vertical scale is not normalized and the ISE amplitude is in arbitrary units. Note that since there are no pathways which enable population exchange with other energy levels, the ISE curves exhibit a "flat top".

Laser Saturation of a Transition

Figures A3 and A4 both exhibit the phenomenon of laser "saturation of a transition", viz, the ISE does not increase indefinitely with laser power but instead approaches an asymptotic value. We shall now investigate this phenomenon and its practical consequences.

Consider solution (5) of the differential equation (3) for the upper of the laser coupled levels. Under saturation conditions we may write

$$R_{ij} + R_{ji} \gg N_e(K_{ij} + K_{ji}) + A_{ji} + D_i + D_j \qquad (12)$$

In which case the solution (5) takes the form

$$N_j(t) = C/B + E_1 e^{-t/\tau_P} + E_2 e^{-t/\tau_F} \qquad (13)$$

where

$$\tau_P \approx [(1 + g)R_{ji}]^{-1} \qquad (14)$$

and

$$\tau_F \approx \frac{(1 + g)}{D_i + gD_j} \tag{15}$$

where we have used the general relation

$$g_i R_{ij} = g_j R_{ji} \tag{16}$$

and have defined

$$g = g_j/g_i \tag{17}$$

as the ratio of degeneracies of the two laser coupled levels. These results are the same as obtained originally by the author.[1] Note that the requirement (12) implies that $\tau_P \ll \tau_F$.

τ_P is the characteristic time for laser induced redistribution of the populations in levels i and j (the laser pumping time), and τ_F is the relaxation time of the system in the presence of the laser radiation field.

Under conditions of laser saturation

$$\frac{dN_j}{dt} \approx N_i R_{ij} - N_j R_{ji} \tag{18}$$

and for the time domain; $\tau_P < t < \tau_F$, we can write

$$N_j/N_i \approx g_j/g_i \tag{19}$$

This radiative balance condition corresponds to an equivalent infinite temperature.

If we now restrict our attention to the C-branch of Fig. A2 (i.e., $Q > 1$ and $s < 1$) then, as first shown by Measures (1968), (19) applies at the time where N_j is a maximum. Consequently, for times $< \tau_F$, we can invoke continuity to provide

$$N_j(t) + N_i(t) = N_j(0) + N_i(0) \tag{20}$$

where $t = 0$ refers to the time just prior to laser irradiation, and arrive at the population enhancement ratio:

$$\frac{N_j^{max}}{N_j(0)} = \left(1 + \frac{N_i(0)}{N_j(0)}\right)\left(1 + \frac{g_i}{g_j}\right)^{-1} \tag{21}$$

Thus by observing the change in spontaneous emission resulting from the sudden application of a saturating laser pulse, we can evaluate $N_i(0)/N_j(0)$. Under conditions of thermal (or collisional) equilibrium this ratio can be used to derive the temperature T_o prior to laser irradiation since T_o is related to this population ratio through the Boltzmann relation

$$N_j(0)/N_i(0) = g \exp(-E_{ji}/kT_o) \tag{22}$$

where E_{ji} represents the energy difference between levels j and i.

If the gas has a degree of ionization in excess of a few percent, then T_o is probably equivalent to T_e, the free electron temperature.

Note that in general we can write

$$N_j^{max} = GN_o \tag{23}$$

where

$$G = \frac{g_j}{g_i + g_j} \tag{24}$$

and $N_o = N_i(0) + N_j(0)$. On the other hand, if $N_j(0) \ll N_i(0)$, then (23) still applies but now $N_o = N_i(0)$ and it follows from (23) that the population of any two levels can be compared by laser saturation of the two appropriate transitions.

In general

$$R_{ji} \equiv \frac{B_{ji}}{4\pi} \int I^{\ell}(\nu) \mathcal{L}_{ji}(\nu) d\nu \tag{25}$$

where $\mathcal{L}_{ji}(\nu)$ is the line profile function and $I^{\ell}(\nu)$ represents the laser spectral irradiance. B_{ji} represents the Milne stimulated emission coefficient.

If we assume that the laser is broadband relative to the absorption line width and that the centre frequencies of the two are coincident, we can write

$$\int I^{\ell}(\nu) \mathcal{L}_{ji}(\nu) d\nu \rightarrow I_s^{\ell}$$

where I_s^{ℓ} is the laser spectral irradiance (Wcm^{-2} Hz^{-1}) corresponding to the peak value of the $I^{\ell}(\nu)$ curve. For laser saturation we have seen (12) that

$$R_{ij} + R_{ji} \gg \frac{1}{\tau_i} + \frac{1}{\tau_j} \tag{26}$$

where

$$\frac{1}{\tau_i} = N_2 K_{ij} + D_i \quad \text{and} \quad \frac{1}{\tau_j} = N_e K_{ji} + A_{ji} + D_j$$

Consequently if we define the "saturated spectral irradiance"

$$I_{so} = \frac{8\pi h\nu^3}{(1+g)c^2} \tau_{ji} \left(\frac{1}{\tau_i} + \frac{1}{\tau_j} \right) \tag{27}$$

We can see that the saturation condition implies that

$$I_s^{\ell} \gg I_{so} \tag{28}$$

In Fig. A4, which shows the ISE curve for the special case of resonance pumping, the particular curve corresponding to $I_s^{\ell} = I_{so}$ has been identified by the symbol I_{s8}, which for the case of sodium D_1 resonance line equals 3.5×10^{-10} Wcm^{-2} Hz^{-1}. For a laser with a bandwidth of about 0.005 nm this corresponds to an irradiance I^{ℓ} of about 1.5 Wcm^{-2}. Note that in the case of Fig. A4 we have set $D_i = D_j = 0$ and we have assumed $N_e = 0$.

System Relaxation

On extinguishing the laser radiation, the populations of the various energy levels will redistribute to form a new equilibrium distribution. We now investigate the characteristics of this relaxation as a function of the various system parameters for a step function termination of the laser radiation. The differential equation (3) for $N_j(t)$ still holds, but now R_{ij} and R_{ji} must be set to zero in the equations (4) for the coefficients A, B and C of the differential equation.

Under these circumstances E_1 and E_2 of the solution (5) will be defined by the populations N_i and N_j at the moment the laser radiation terminates. For the general case, the decay characteristic of N_j is a complex function of the system parameters, but for the case of $N_e(K_{ij} + K_{ji}) + A_{ji} \gg D_i + D_j$, the decay rates $\lambda_{1,2}$ take on simple forms:

$$-\lambda_1 \approx B/A \ll 1$$

$$-\lambda_2 \approx A \gg 1$$

where

$$A \approx N_e(K_{ij} + K_{ji}) + A_{ji} \tag{29}$$

If further we assume $D_i = D_j = 0$ and consequently $C_i = C_j = 0$, then the form of the differential equation (3) changes to first order with a solution

$$N_j(t) = E_3 e^{\lambda_3 t} + E_4 \tag{30}$$

where

$$\lambda_3 = -[N_e(K_{ij} + K_{ji}) + A_{ji}] \tag{31}$$

and where E_3 and E_4 are constants which can be related to conditions prior to irradiation. The important thing to note is that the time constant for relaxation of the population in level j

$$\tau_3 = -\lambda_3^{-1} \tag{32}$$

and therefore the decay characteristic of the ISE can be used to calculate N_e if K_{ij} and K_{ji} are known along with A_{ji}. This assumes that radiation trapping can be safely ignored. If $N_e = 0$, then

$$\tau_3 = A_{ji}^{-1} \tag{33}$$

and the lifetime of the upper state can be measured directly. Note that if alternative radiative decay modes exist for the laser enhanced population, we can choose to monitor the ISE at a wavelength other than the laser wavelength, thereby eliminating Rayleigh, Mie, and apparatus scattering. In this case, however, (33) must be replaced by

$$\tau_3 = \left(\sum_i A_{ji}\right)^{-1} \tag{34}$$

where the sum extends over all allowed transitions from level j. Transition probabilities can be determined from such measurements if the branching ratios are also evaluated.

REFERENCES

1. R. M. Measures, J. Appl. Phys. 39, 5232, 1968.
2. A. B. Rodrigo and R. M. Measures, IEEE J. Quant. Electr. QE-9, 972, 1973.
3. R. A. Van Calcar, M. J. M. Van de Ven, B. K. Van Uitert, K. J. Biewenga, Tj. Hollander and C. Th. J. Alkemade, J. Quant. Spectrosc. Rad. Transfer, 21, 11, 1979.
4. D. W. Koopman, T. J. McIlrath and V. P. Myerscough, J. Quant. Spectrosc. Rad. Transfer, 19, 555, 1978.
5. R. M. Measures, N. Drewell and H. S. Kwong, Phys. Rev. A, 16, 1093, 1977.
6. T. J. McIlrath and J. L. Carlsten, Phys. Rev. A, 6, 1091, 1972.
7. D. D. Burgess and C. H. Skinner, J. Phys. B. Atom & Molec. Phys. 7, 1297, 1974.
8. R. M. Measures, J. Quant. Spectrosc. Rad. Transfer 10, 107, 1970.
9. A. L. Waksberg and A. I. Carswell, Appl. Phys. Lett. 6, 137, 1965.
10. M. H. Dunn and A. Maitland, Proc. Phys. Soc. 92, 1106, 1967.
11. A. S. Khaikin, Sov. Phys. JETP 24, 25 1967.

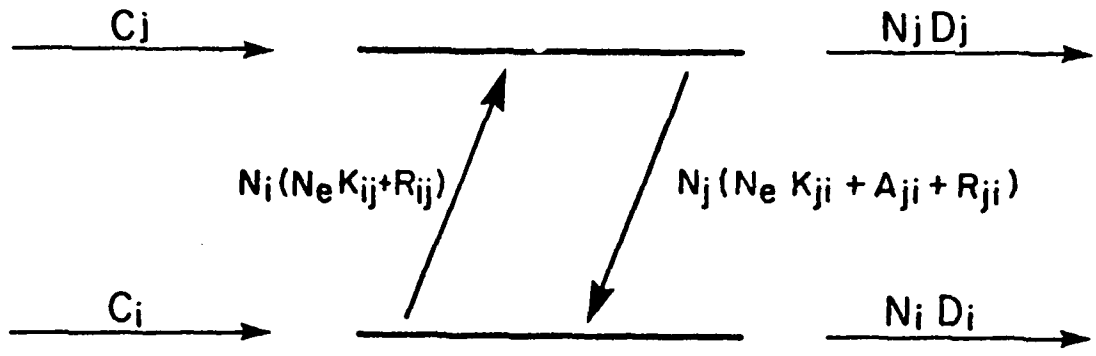

FIG. A1 PARTIAL ENERGY LEVEL DIAGRAM OF AN ATOM SHOWING THE TWO LASER-COUPLED LEVELS.

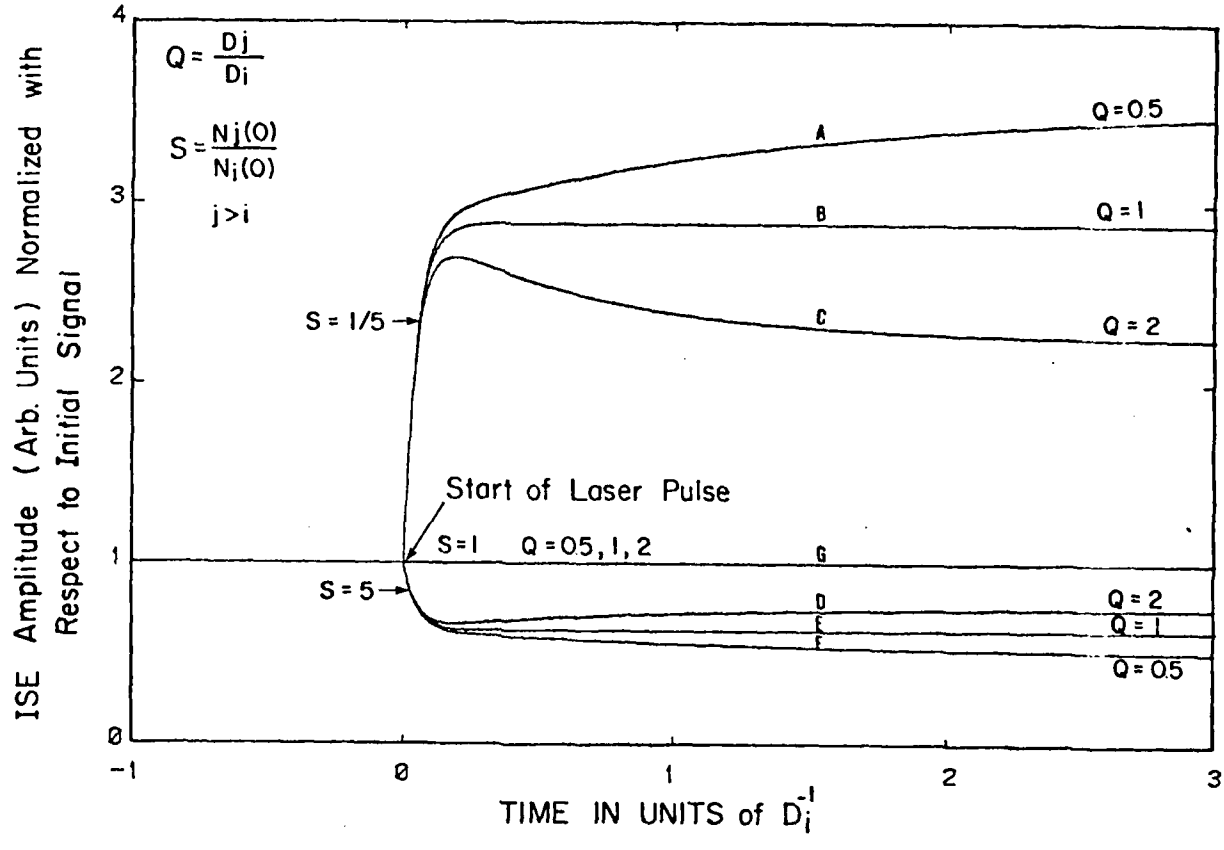

FIG. A2 ISE CURVES UNDER VARIOUS PLASMA CONDITIONS.

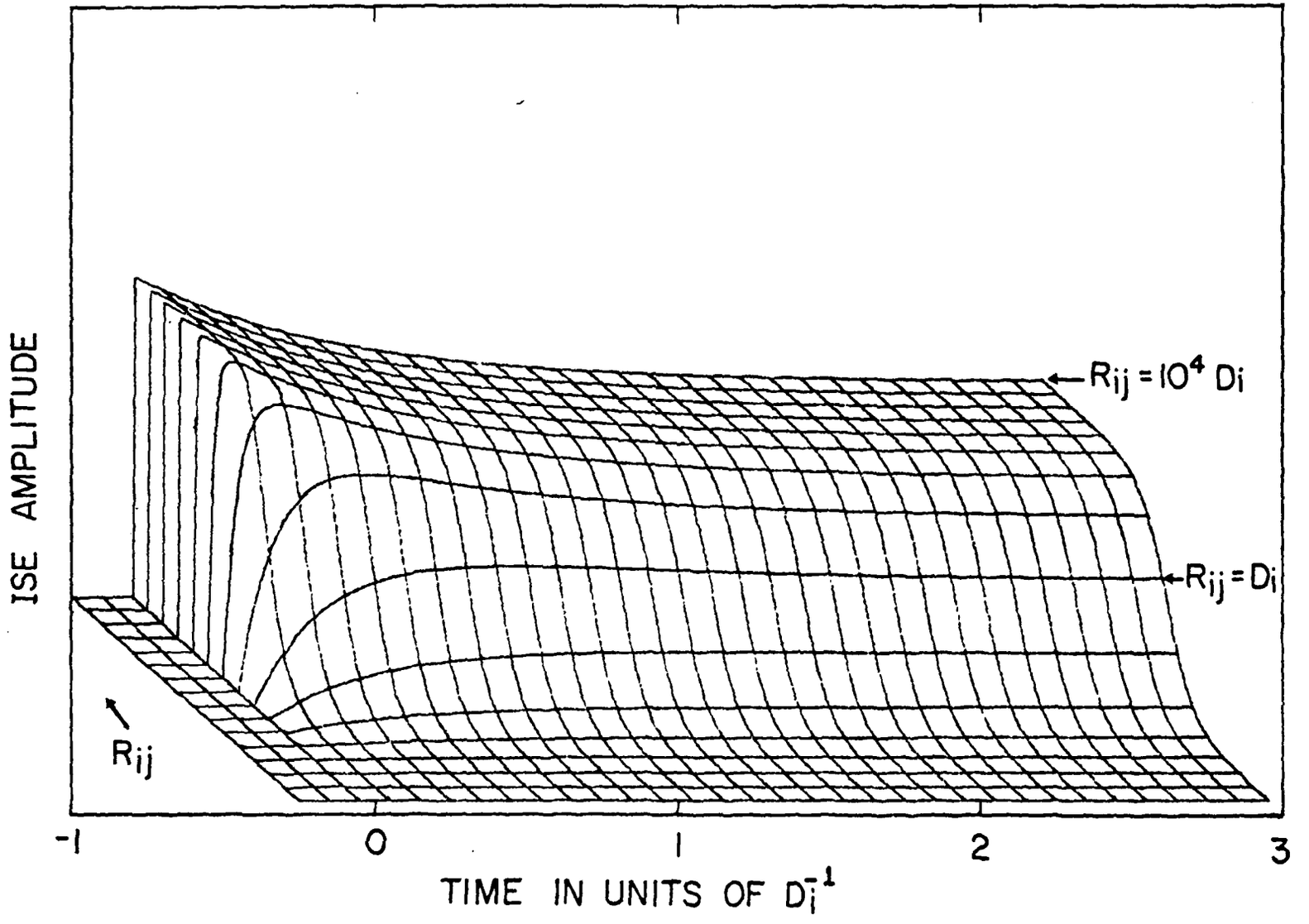

FIG. 43 ISE CURVES FOR VARIOUS LASER POWERS.

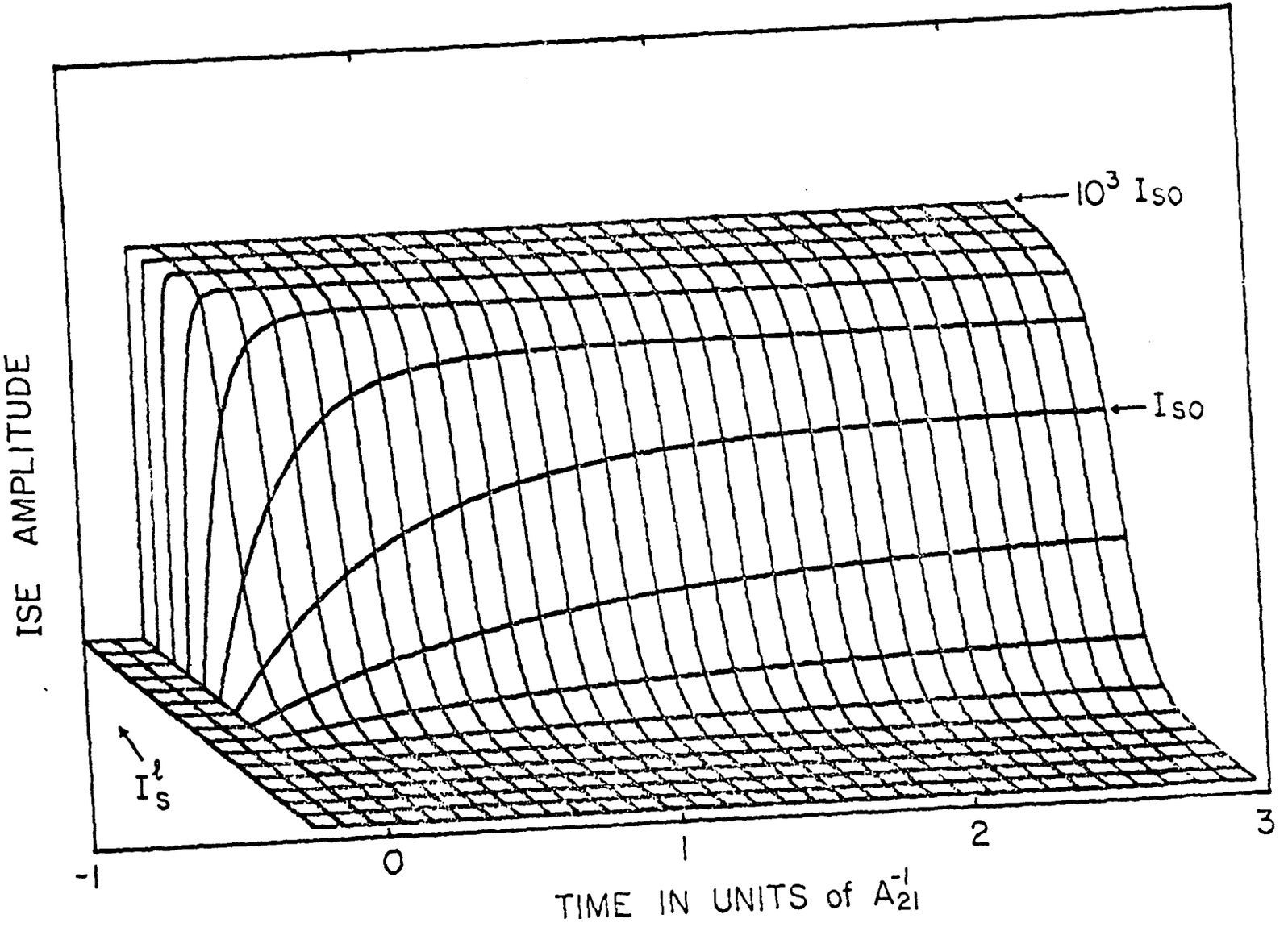

FIG. A-1 ISE CURVES FOR RESONANCE PUMPING AT VARIOUS LASER POWERS.

Appendix B

FAST AND EFFICIENT PLASMA HEATING THROUGH SUPERELASTIC LASER ENERGY CONVERSION (SELEC)

R. M. Measures*, P. L. Wizinowich and P. G. Cardinal

Institute for Aerospace Studies
University of Toronto
4925 Dufferin Street
Downsview, Ontario, Canada
M3H 5T6

ABSTRACT

Superelastic laser energy conversion, SELEC, has been shown to be capable of extremely rapid rates of plasma heating with relatively modest values of laser irradiance. In the case of a boron III plasma, $dT_e/dt > 10^{13}$ °K sec^{-1} has been predicted for an initial BIII ion density of 10^{17} cm^{-3}. The laser irradiance needed to achieve this rate of change of the free electron temperature is about 5×10^8 Wcm^{-2} per cm of path length.

---

*Professor of Applied Science and Engineering, University of Toronto.

INTRODUCTION

Laser saturation of a resonance transition has long been recognized[1] as a very effective means of coupling laser energy into a gaseous medium. In essence the dense population of resonance state atoms resulting from laser saturation represent both a source of energy for rapidly heating the medium[1,2] and a large pool of atoms having their ionization energy reduced by the laser photon energy. In the case of an un-ionized gas, this interaction is predicted to rapidly create almost full ionization,[3,4] in accordance with recent experimental observations.[5,6]

We have recently proposed that this LIBORS (Laser Interaction Based On Resonance Saturation) technique[4] should be ideal for producing the long plasma channels required for the transport of electron (or light ion) beams in proposed new approaches at inertial fusion.[7,8] We have also shown that this method of coupling laser energy into a plasma has several advantages over inverse bremsstrahlung.[9]

The purpose of the present work is to indicate the degree of plasma heating that can be achieved through superelastic laser energy conversion (SELEC). In order to generalize this plasma heating mechanism as far as possible we have developed a two parameter model of the laser pumped species. We also show that this model, albeit very simple, predicts a temperature increase that is in reasonable agreement with the results of our extensive LIBORS computer code.[4] We show that a substantial increase in the electron temperature can be achieved with a suitable choice of ion species, and that the time for this temperature jump can be very short at high densities - a feature that is quite conducive to the development of short wavelength lasers.[10] Indeed, in the case of a Boron III plasma we predict that a heating rate in excess of 10^{13} °K sec^{-1} should be attainable within a column of 2 mm width for a laser irradiance of about 10^{8} Wcm^{-2}.

SIMPLE SELEC MODEL FORMULATION

It is necessary at the outset to clarify the difference between SELEC and LIBORS, for both involve laser saturation of a resonance transition. SELEC refers to the rapid electron heating that occurs prior to an appreciable increase in the free electron density, whereas LIBORS refers to the entire interaction that includes close to complete burn out of the particular ion species being pumped.

In general the superelastic heating rate of the free electrons can be expressed in the form

$$Q_{SE} = N_e N_2 K_{21} E_{21} \qquad (1)$$

where N_e represents the free electron density (cm^{-3}),

N_2 represents the resonance state population density of the laser pumped ion (LPI) (cm^{-3}),

K_{21} represents the superelastic collision rate coefficient for the laser saturated transition (cm^3 sec^{-1}), and

E_{21} represents the resonance to ground state energy difference for the LPI (J).

We shall restrict our attention to a highly ionized plasma in which the LPI constitutes the dominant species. Furthermore, we shall first consider the energy level structure of the LPI to be well represented by a two level system. In which case the electron energy equation takes the form

$$\frac{d}{dt}\left(\frac{3}{2}kT_e\right) \simeq N_2K_{21}E_{21} - N_1K_{12}E_{21} \qquad (2)$$

where $\frac{3}{2}kT_e$ represents the mean translation energy per electron, assuming a Maxwell-Boltzmann distribution, and K_{12} represents the electron collision rate coefficient for excitation of the resonance transition.

Measures[11] has shown that under laser saturation conditions the redistribution of the population between the two laser coupled states occurs in a time approximately given by

$$\tau_s \simeq \frac{1}{(1+g)R_{21}} \qquad (3)$$

where $g = g_2/g_1$, the ratio of the degeneracies of the two levels and

$R_{21} = \frac{B_{21}}{4\pi}\int I^L(\nu)f_{21}(\nu)d\nu$ represents the stimulated emission rate,

B_{21} is the Milne stimulated emission coefficient, $I^L(\nu)$ is the laser spectral irradiance and $f_{21}(\nu)$ the line profile function.

For strong saturation conditions, this redistribution occurs in a time that is very short compared to any other characteristic time of interest. Consequently, we can assume that the ratio of the resonance to ground state populations is given by

$$\frac{N_2}{N_1} \simeq \frac{R_{12} + N_eK_{12}}{R_{21} + A_{21} + N_eK_{21}} \qquad (4)$$

where A_{21} represents the Einstein spontaneous transition probability and

$$R_{12} = gR_{21} \qquad (5)$$

If we incorporate equation (4) in (2) we can obtain

$$\frac{d}{dt}\left(\frac{3}{2}kT_e\right) \simeq \frac{N_2K_{21}E_{21}R_{12}}{(R_{12}+N_eK_{12})}\left[1 - \frac{(R_{21}+A_{21})K_{12}}{R_{12}K_{21}}\right] \qquad (6)$$

From consideration of detailed balance,

$$K_{12} = gK_{21}\exp(-E_{21}/kT_e) \qquad (7)$$

and so we may write

$$\frac{d}{dt}\left(\frac{3}{2}kT_e\right) \simeq \frac{N_2K_{21}E_{21}}{(1+N_eK_{12}/R_{12})}\left[1 - \left\{1 + \frac{A_{21}}{R_{21}}\right\}\exp(-E_{21}/kT_e)\right] \qquad (8)$$

The electron temperature is seen to increase monotonically towards the asymptotic value given by

$$kT_e^{max} \simeq \frac{E_{21}}{\ln\left[1 + \frac{A_{21}}{R_{21}}\right]} \qquad (9)$$

for which $d/dt(kT_e) \simeq 0$. If we assume that $A_{21} \ll R_{21}$, i.e., strong saturating conditions, then we can write

$$kT_e^{max} \simeq \frac{R_{21}}{A_{21}}E_{21} \qquad (10)$$

For broad band laser radiation,

$$R_{21} = \frac{B_{21}}{4\pi}\int I^L(\nu)f_{21}(\nu)d\nu \simeq \frac{I^L(\nu)}{h\nu}\sigma_{21} \qquad (11)$$

where

$$\sigma_{21} = \frac{h\nu}{4\pi}\int B_{21}\phi_{21}(\nu)d\nu \qquad (12)$$

and represents the frequency integrated stimulated emission cross section. We can then introduce the "saturated spectral irradiance"

$$I_s = \frac{h\nu}{\sigma_{21}\tau_{21}^{RAD}} \qquad (13)$$

where

$$\tau_{21}^{RAD} = 1/A_{21}$$

and write

$$kT_e^{max} \simeq E_{21} I^{\ell}(\nu)/I_s \qquad (14)$$

Clearly, this can represent a significant temperature under strong saturation conditions, where, $I^{\ell}(\nu) \gg I_s$.

In the case of any real ion, collisional excitation to levels above the resonance level will constitute an additional loss term in the free electron energy equation. Indeed, it is the collisionally induced upwelling of the resonance state population that eventually leads to ionization burn out of the species being pumped. In the SELEC regime (corresponding to times short compared to the ionization burn out time of the LPI), the energy equation takes the form

$$\frac{3}{2}\frac{d}{dt}(kT_e) \simeq N_2 K_{21} E_{21} - N_1 K_{12} E_{21} - \sum_{\substack{m>2 \\ p=1,2}} N_p K_{pm} E_{mp} + \sum_{\substack{m>2 \\ p=1,2}} N_m K_{mp} E_{mp} \qquad (15)$$

The last term on the RHS of equation (15) represents an additional heating term due to superelastic collisional quenching of the higher excited states ($m > 2$). Obviously, this term only becomes significant once the population in these excited states approaches the equilibrium value corresponding to the instantaneous free electron temperature.

Clearly, if SELEC is to induce as large a temperature jump as possible [the limiting value being given by equation (14)] the third term on the RHS of equation (15) should be as small as possible. This suggests that the energy difference between the resonance level and the next excited level ($m = 3$) should be as large as possible in comparison with the energy difference between the laser coupled levels, viz.,

$$E_{32} \gg E_{21}$$

In order to represent the LPI by a two parameter model we shall use the 3 level system* shown in figure 1. It should be noted that we have also found it possible to approximate the ionization time of a cold vapor subjected to laser resonance saturation by a simple model.[2] We collapse all the higher levels ($m > 3$) into a single manifold and assume a net rate of loss of population from $m = 3$ to this manifold given by $N_e N_3 C_3$.

Under conditions of strong laser saturation of the resonance transition, the resonance and ground state populations are approximately locked together in the ratio of their degeneracies,[11] i.e.,

$$\frac{N_2}{N_1} \simeq \frac{g_2}{g_1} = g \qquad (16)$$

which corresponds to an infinite temperature distribution. For most species $g > 1$ and the resonance state will have the greater population. Furthermore,

*It should be realized, however, that the 3rd level in the model need not necessarily correspond to the 3rd excited state. If several intermediate levels lie close together, either the one with a much larger collision cross section is chosen, or the group is treated as the 3rd level.

since $K_{1m} << K_{2m}$ collisional cooling arising from ground state excitation to m (> 2) levels is neglected in this model.

We shall consider two limiting situations:

(A) $$N_e N_3 C_3 >> N_e N_3 K_{32} + N_3 A_{32}$$

or

(B) $$N_e N_3 K_{32} + N_3 A_{32} >> N_e N_3 C_3$$

In case (B), the intermediate population has to be taken into account as its finite value leads to additional superelastic collisions. This model requires the solution of three rate equations and the introduction of a 3rd parameter: $\gamma = N_e C_3/(N_e K_{32} + A_{32})$. We have shown elsewhere[12] that this more complicated model overpredicts the increase in T_e compared to the results of the full LIBORS code, except for large values of γ (> 20). Under these circumstances the solutions for $T_e(t)$ are quite well approximated by the simpler two parameter model referred to as case (A). Consequently, for the remainder of this paper we shall restrict our attention to a comparison of the simple 2 parameter model with that of the full LIBORS code.

In case (A), we can evaluate the time history of the electron temperature simply by solving the appropriate energy equation,

$$\frac{3}{2}\frac{d}{dt}(kT_e) = N_2 K_{21} E_{21} - N_1 K_{12} E_{21} - N_2 K_{23} E_{32} \qquad (17)$$

In this instance the collision rate to the manifold is so great that we can neglect the population build-up in the intermediate(m = 3)state. This

"infinite sink" model will tend to underestimate the rise in T_e, as we neglect the downward collisions that tend to reduce the effective cooling effect of collisional excitation.

We shall assume Seaton type collision rate coefficients[13] so that we may write

$$K_{23} = \frac{A\bar{f}_{23}}{E_{32}\sqrt{kT_e}} \exp(-E_{32}/kT_e) \qquad (18)$$

and

$$K_{12} = \frac{A\bar{f}_{12}}{E_{21}\sqrt{kT_e}} \exp(-E_{21}/kT_e) \qquad (19)$$

where

$$\bar{f}_{mn} = f_{mn}\langle\bar{g}\rangle_{mn} \qquad (20)$$

f_{mn} being the absorption oscillator strength and $\langle\bar{g}\rangle_{mn}$ the effective Gaunt factor for the mn transition ($A = 1.6 \times 10^{-5}$). If we now introduce the two "fitting parameters",

$$a = E_{32}/E_{21} \text{ and } b = \bar{f}_{12}/a\bar{f}_{23}$$

and a nondimensional temperature

$$\theta = kT_e/E_{21}$$

we can rewrite equation (17) in the form

$$\frac{d\theta}{dt} = \frac{2}{3} N_2 K_{21}[1 - \exp(-1/\theta) - \exp(-a/\theta)/b] \qquad (21)$$

We see that $d\theta/dt = 0$ leads to a transcendental equation for θ, i.e., the steady state temperature,

$$\theta_s = \frac{a}{\ln\left[\frac{1}{b(1 - \exp(-1/\theta_s))}\right]} \qquad (22)$$

For $\theta_s \geq 1$, we can arrive at an approximation to θ_s in terms of the two parameters, viz.,

$$\theta_s \simeq -\frac{a}{\ln[b(1 - \exp(\ln b/a))]} \qquad (23)$$

The transcendental equation (22) has been solved and the results presented in figure 2, where this steady state temperature, θ_s, is plotted as a function of "a" for several values of "b".

If the initial value of the electron temperature is greater than this steady state value, i.e., $\theta_o > \theta_s$, then in fact SELEC produces a "cooling effect" and a rapid drop of T_e is predicted. This may appear to be a paradox, but in fact has a sound physical explanation. If $\theta_o > \theta_s$, then initially

$$N_2 K_{21} E_{21} < N_1 K_{12} E_{21} + N_2 K_{23} E_{32} \qquad (24)$$

due to the large values of K_{12} and K_{23}. Consequently the electron temperature is reduced at the expense of raising the population from level 2 to level 3.

If we introduce the nondimensional time,

$$\tau = \frac{2}{3} N_2 K_{21}^* t \simeq \frac{2}{3} G N_o K_{21}^* t \qquad (25)$$

where N_o represents the ground state density of the LPI prior to laser saturation [assuming $N_2(0)/N_1(0) \ll 1$],

$$G = g/(1 + g)$$

and

$$K_{21}^* = \frac{A\bar{f}_{12}}{gE_{21}^{3/2}} (= K_{21} \quad \text{for } \theta = 1)$$

the free electron energy equation can be expressed in the nondimensional form

$$\frac{d\theta}{d\tau} = \frac{1}{\sqrt{\theta}} [1 - \exp(-1/\theta) - \exp(-a/\theta)/b] \qquad (26)$$

In most cases of interest for heating, we can assume that $\theta_o < 1$, in which case the initial temperature gradient can be approximated by the expression,

$$\frac{d\theta}{d\tau} \simeq \frac{1}{\sqrt{\theta}} \qquad (27)$$

which in essence states that for early times the rate of change of free electron temperature is dominated by the resonance superelastic heating term, or

$$\left.\frac{dT_e}{dt}\right|_o = \frac{2}{3k} G N_o K_{21}(T_{eo}) E_{21} \qquad (28)$$

A simple estimate of the time to produce a significant increase in the free electron temperature can be obtained in the following manner. Integration of equation (27) yields

$$\theta \simeq [\theta_o^{3/2} + 3\tau/2]^{2/3} \qquad (29)$$

Consequently, we can write the SELEC heating time

$$t_H^* \simeq [\theta_s^{3/2} - \theta_o^{3/2}]/GN_oK_{21}^* \qquad (30)$$

Under conditions of strong saturation of a resonance transition within a plasma, Measures[1,4] has shown that the attenuation of the laser beam is primarily determined by superelastic dissipation, viz.,

$$\frac{d}{dx} I^{\ell}(x) = -N_2N_eK_{21}E_{21} \qquad (31)$$

The laser irradiance required to heat a uniform plasma of thickness, L, is given by

$$I^{\ell} \simeq GN_oN_{eo}K_{21}(T_{eo})LE_{21} \qquad (32)$$

LEDOR COMPUTER CODE

In order to ascertain the consequences of strongly saturating one of the resonance transitions within a major constituent of a plasma we have represented the laser excited species by a multilevel model and solved the appropriate set of energy transport and collisional-radiative population

rate equations. A rate equation analysis is applicable in the present paper because of the high density conditions (short dephasing time[14]) assumed. The general rate equation that describes the temporal variation of the population density of level n (n > 2) can be expressed in the form

$$\frac{dN_n}{dt} = N_e\sum_{m\neq n} N_mK_{mn} + \sum_{m>n} N_mA_{mn}^* + N_e^2N_zK_{cn} + N_eN_z\beta(n) - N_n\left[N_e\sum_{m\neq n} K_{nm} + \sum_{m<n} A_{nm}^* + \alpha_{nc}I^{\ell} + N_eK_{nc}\right] \qquad (33)$$

where A_{mn}^* ($=q_{mn}A_{mn}$) (sec^{-1}) is the spontaneous emission probability for m to n transition allowing for radiation trapping through the use of the Holstein escape factor,[15] q_{mn},

N_n (cm^{-3}) represents the population density of level n in LPI (effective charge z - 1),

N_z (cm^{-3}) represents the ion density of the next ionization stage, effective charge z,

$\beta(n)$ ($cm^3\ sec^{-1}$) represents the radiative recombination rate coefficient[16],

α_{nc} ($cm^2\ J^{-1}$) represents the hydrogen-like single photon ionization rate coefficient for level $n > n^*$, for $E_{cn} < E_{21}$,

I^{ℓ} (Wcm^{-2}) represents the laser irradiance ($I^{\ell} = \int I^{\ell}(\nu)d\nu$)

K_{cn} ($cm^6\ sec^{-1}$) represents the three body recombination rate coefficient,

K_{nc} ($cm^3\ sec^{-1}$) the electron collisional ionization rate coefficient,

K_{mn} ($cm^{-3}\ sec^{-1}$) represents the mn transition electron collisional rate coefficient and is calculated on the basis of Seaton cross-sections for optically allowed transitions[13] and Gryzinsky cross-sections[16] for others.

The appropriate electron energy equation takes the form

$$\frac{d}{dt}\left[\frac{3}{2}N_e kT_e\right] = N_2 N_e K_{21} E_{21} + N_e^2 N_z \sum K_{cn} E_{cn} + \sum_{n>n^*}(E_{21} - E_{cn})\alpha_{nc} I^{\ell}$$

$$- N_e \sum_{n\geq 1} N_n K_{nc} E_{cn} - N_e C - N_e[N_z H_{ei}^z + N_{z-1} H_{ei}^{z-1}]$$

$$- \frac{3}{2} N_e N_z kT_e \sum_{n\geq 1} B(n) \qquad (34)$$

where

$$C = \sum_{n\geq 1}\sum_{m>n}(N_n K_{nm} - N_m K_{mn})E_{mn} + N_2 K_{21} E_{21} \qquad (35)$$

and represents the average loss of energy per electron due to the net collisionally induced upward movement of the bound electrons. H_{ei}^z represents the rate of elastic energy transfer to ion species with effective charge z through Coulomb scattering collisions,[17] viz.,

$$H_{ei}^z = \frac{z^2 e^4}{m_i}\left(\frac{8\pi m_e}{kT_e}\right)^{\frac{1}{2}} \frac{T_e - T_i}{T_e} \ln\left[\frac{9(kT_e)^3}{8\pi N_e z^2 e^6}\right] \qquad (36)$$

This set of equations is solved by a Runge-Kutta technique assuming a step-like laser pulse with instantaneous saturation at t = 0. The plasma is assumed to be in Local Thermodynamic Equilibrium at temperature, T_{eo}, prior to laser irradiation. The LIBORS code evaluates the temporal development of (i) each of the atomic level populations used to represent the LPI, (ii) the free electron density and temperature, (iii) the ion temperature and (iv) the laser power absorbed per unit length of the laser beam. Further details of the LIBORS computer code are provided by Cardinal,[3] Measures et al,[4] and Drewell.[18]

SELECTION FOR A BORON III PLASMA

Reference to the partial (Grotrian) energy level diagram for BIII, figure 3, clearly reveals the large energy separation between the resonance level and the next group of excited levels relative to the resonance to ground energy separation. Consequently a plasma which has doubly ionized boron

(BIII) as the dominant species should be quite suitable for superelastic heating through laser resonance saturation. The oscillator strengths and energies of the most important transitions for BIII are listed in table I. From this we determine that for BIII the energy level ratio, "a" = E_{52}/E_{21} = 3.05 and the collision rate ratio, "b" = $\bar{\Gamma}_{12}/g\bar{\Gamma}_{25}$ = 0.187, viz., we have chosen the intermediate level to be level 5, since the 2-5 transition has a much larger oscillator strength than the other possible choice, 2-3.

If these values of a and b are used in equation (23), we deduce that $\theta_s \simeq 1.20$ (i.e., $T_e^{max} \sim$ 83,400°K) and that the heating times, as given by equation (30), are

$t_H^* \sim 0.5$ nsec, for N_o(BIII) = 10^{17} cm^{-3}, T_{eo} = 32,000°K

$t_H^* \sim 5.3$ nsec, for N_o(BIII) = 10^{16} cm^{-3}, T_{eo} = 27,000°K

$t_H^* \sim 56.3$ nsec, for N_o(BIII) = 10^{15} cm^{-3}, T_{eo} = 23,000°K

The initial free electron temperatures T_{eo} were established by requiring that the plasma had the indicated BIII ion density and that this species dominated (by about an order of magnitude) both BII and BIV ion densities, assuming LTE.

The free electron temperature time histories subsequent to laser resonance saturation, as calculated by the simple model equation (26) are presented as figure 4. It can be seen that the temperature and heating times predicted by equations (23) and (30) are in reasonable agreement with the results seen in figure 4. Furthermore, at an ion density of 10^{17} cm^{-3}, and an initial temperature of 32,000°K, equation (28) predicts a heating rate of about 1.4×10^{14}°K sec^{-1} while equation (32) predicts a required laser irradiance of about 2.84×10^8 Wcm^{-2} per cm path.

A more reliable set of predictions of the superelastic heating of a boron III plasma has been obtained by treating BIII as a 14-level ion, see figure 3, in our extensive LIBORS computer code. The temporal variation of: the free electron temperature T_e, the free electron density N_e, the ion temperature, T_i, the population density of the key intermediate level, N_5(BIII) and the laser

irradiance absorbed per cm path length ζ^{ℓ}, are presented as figure 5 for a plasma assumed to be initially in LTE with $N_o(BIII) = 10^{16}$ cm^{-3}, $N_{eo} = 2 \times 10^{16}$ cm^{-3} and $T_{eo} = 27{,}000$°K.

The electron temperature can be seen to double within 4 nsec, which corresponds to a heating rate of about 8×10^{12} °K sec^{-1}, and reaches a plateau value of about 73,000°K in close to 10 nsec. The peak laser irradiance absorbed is about 5.7×10^{6} Wcm^{-2} per cm path length and is seen to rapidly drop at first due to the sudden rise in the free electron temperature. Significant ionization of the BIII ion is observed to occur after 15 nsec - as seen by the increase in N_e and the decrease in N_5(BIII).

A comparison of the heating rates for three initial BIII-ion densities [$N_o(BIII) = 10^{17}$, 10^{16} and 10^{15} cm^{-3}] can be obtained by reference to figure 6. This set of LIBORS code electron temperature histories can be seen to compare quite favourably to the predictions of the simple model equation (26) as portrayed in figure 4.

For the highest density plasma, $N_o(BIII) = 10^{17}$ cm^{-3}, figure 6, SELEC is seen to produce a heating rate, $dT_e/dt \simeq 4 \times 10^{13}$ °K sec^{-1}. Furthermore, the peak laser irradiance absorbed per cm path length under these conditions is about 4.8×10^{8} Wcm^{-3}, which corresponds to a laser irradiance of only 10^{3} Wcm^{-2} for a plasma of 2 mm thickness.

CONCLUSIONS

We have shown theoretically that the combination of laser saturation of an ion resonance transition with superelastic collision quenching should constitute an extremely rapid and efficient method of heating a plasma. We have developed a simple three level model that enables us to characterize the interaction in terms of two parameters: the energy level ratio, "a" and the superelastic to inelastic collision ratio, "b".

This study reveals that in order to attain the greatest jump in plasma temperature we need to select an ion that possesses as large values of "a" and "b" as possible. Indeed, we have found that the normalized plateau temperature predicted by this superelastic laser energy conversion (SELEC) technique can be approximately given by equation (23),

$$\theta_s = -\frac{a}{\ln[b(1 - \exp(\ln b/a))]} \qquad (23)$$

where $\theta_s = kT_e^{max}/E_{21}$.

The rate of heating and its dependence upon the laser pumped ion density, as predicted by this simple three level model, is found to compare favourably with a much more reliable multilevel computer simulation of the interaction.

This simple three level model also predicts a substantial cooling of the plasma can be achieved by chosing the plasma temperature (prior to laser irradiation) to be larger than the plateau temperature, i.e., $T_{eo} > T_e^{max}$. Indeed, the rate of cooling can be compareble in magnitude to the rate of heating at the same ion density.

In the case of a boron III dominated plasma, the simple model predicts a steady state temperature of about 83,000°K, an initial heating rate of about 1.4×10^{14} °K sec^{-1} and a laser irradiance of 5.7×10^{8} Wcm^{-2} per cm of plasma with an initial BIII ion density of 10^{17} cm^{-3}. These results are seen to compare well with the more extensive LIBORS computer code predictions of 73,000°K, 4×10^{13} °K sec^{-1} and 5×10^{8} Wcm^{-3} respectively.

This work was supported by USAF/AFOSR under grant 76-2902B and the National Science and Engineering Research Council of Canada.

Table I. Simple Model Parameter for BIII

Transition	Wavelength	Energy Separation	Oscillator Strength
$1 \rightarrow 2$	206 nm	5.99 eV	0.366
$1 \rightarrow 4$	51.8 nm	23.91 eV	0.151
$2 \rightarrow 3$	75.9 nm	16.29 eV	0.047
$2 \rightarrow 5$	67.7 nm	18.29 eV	0.651

NB that the energy spacing and relative oscillator strengths for BIII lead to $a = E_{52}/E_{21} = 3.05$ and $b = \bar{f}_{12}/g\bar{f}_{25} = 0.187$. The Gaunt factors for $1 \rightarrow 2$ and $2 \rightarrow 5$ transitions are assumed equal at about 0.2.

REFERENCES

1. R. M. Measures, J. Quant. Spectrosc. Radiat. Transfer 10, 107-125 (1970).
2. R. M. Measures, N. Drewell and P. Cardinal, "Radiation Energy Conversion in Space", Ed. K. W. Billman, Vol. 61, Progress in Astronautics and Aeronautics, 450-464 (1978).
3. P. G. Cardinal (unpublished).
4. R. M. Measures, N. Drewell, P. G. Cardinal, J. Appl. Phys. 50, 2662-2669 (1979).
5. T. B. Lucatorto and T. J. McIlrath, Phys. Rev. Lett. 37, 428-431 (1976).
6. T. J. McIlrath and T. B. Lucatorto, Phys. Rev. Lett. 38, 1390-1393 (1977).
7. G. Yonas, J. W. Poukey, K. R. Prestwick, J. R. Freeman, A. J. Toepfer, and M. J. Clauser, Nucl. Fusion 14, 731-740 (1974).
8. M. J. Clauser, Phys. Rev. Lett. 35, 848-851 (1975; H. M. Fleischmann, Phys. Today, 35-43 (1975).
9. R. M. Measures, N. Drewell, P. G. Cardinal, Appl. Optics, 18, 1824-1827 (1979).
10. T. C. Bristow, M. J. Lubin, J. M. Forsyth, E. B. Goldman and J. M. Soures, Optics Communications, 5, 315-318 (1972).
11. R. M. Measures, J. Appl. Phys. 39, 5232-5245 (1968).
12. P. L. Wizinowich (unpublished).
13. M. J. Seaton, Atomic and Molecular Processes, Ed. D. R. Bates, Academic, New York (1962).
14. T. J. McIlrath and J. L. Carlsten, Phys. Rev. A6, 1091, 1972.
15. T. Holstein, Phys. Rev. 83, 1159 (1951).

FIGURE CAPTIONS

1. Simple three-level model representation of Superelastic Laser Energy Conversion (SELEC)
2. Variation of the normalized plateau temperature with the energy level ratio, "a", for various values of the collision rate parameter, "b", according to the simple SELEC model.
3. Partial Grotrian energy level diagram for boron III.
4. Predicted SELEC free electron heating for a boron III plasma based on the simple model.
5. LIBORS computer code predictions for a boron III plasma, corresponding to the initial conditions, $N(BIII) = 10^{16}$ cm^{-3}, and $T_{eo} = 27{,}000°$ K.
6. LIBORS computer code predicted free electron heating for three initial conditions of a boron III plasma.

16. M. Gryzinski, Phys. Rev. 138, A336 (1965).
17. J. M. Dawson, Phys. Fluids 7, 981-987 (1964).
18. N. Drewell, UTIAS Report No. 229 (unpublished).

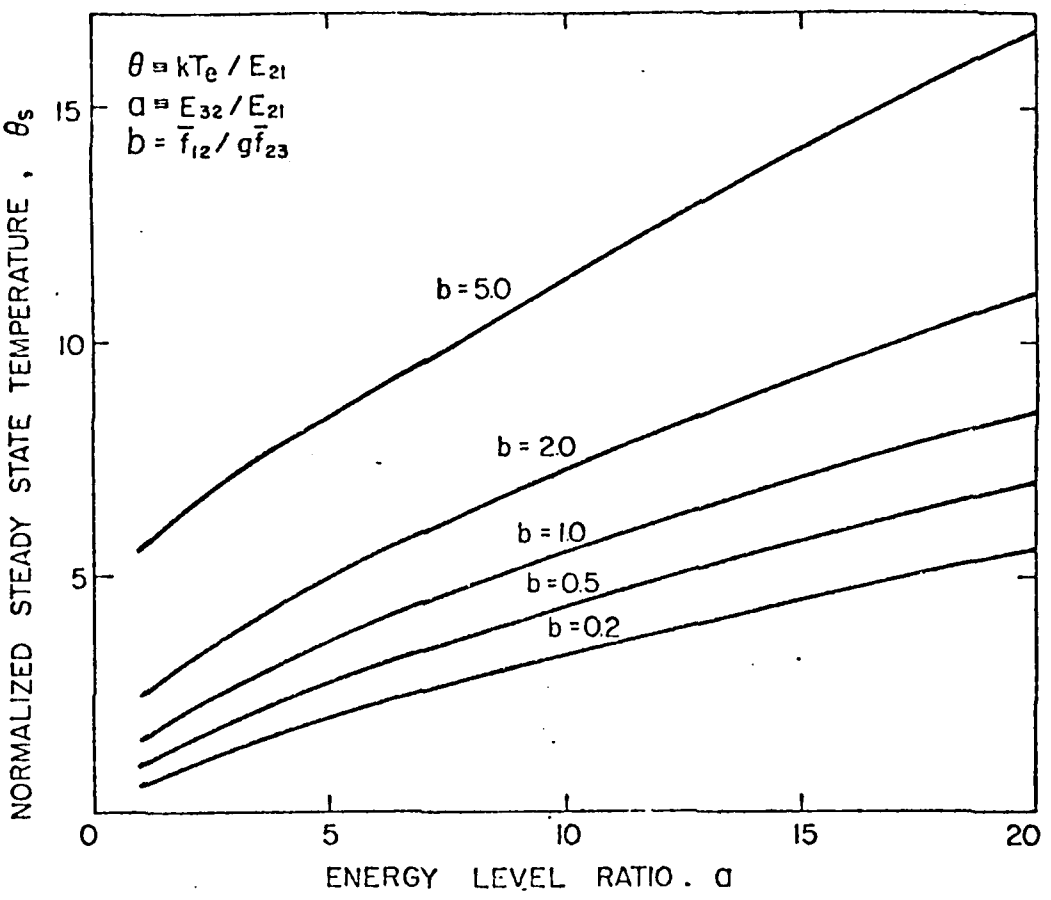

FIG. 2

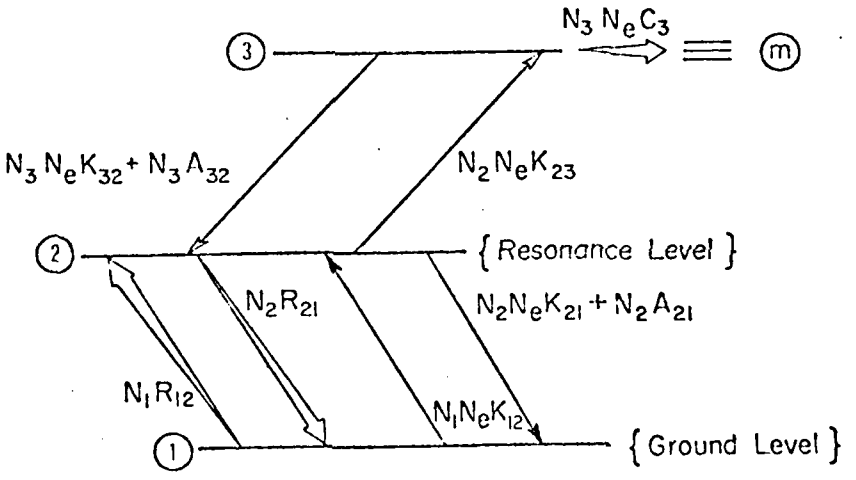

FIG. 1 BASIC PROCESSES INVOLVED IN "SELEC"

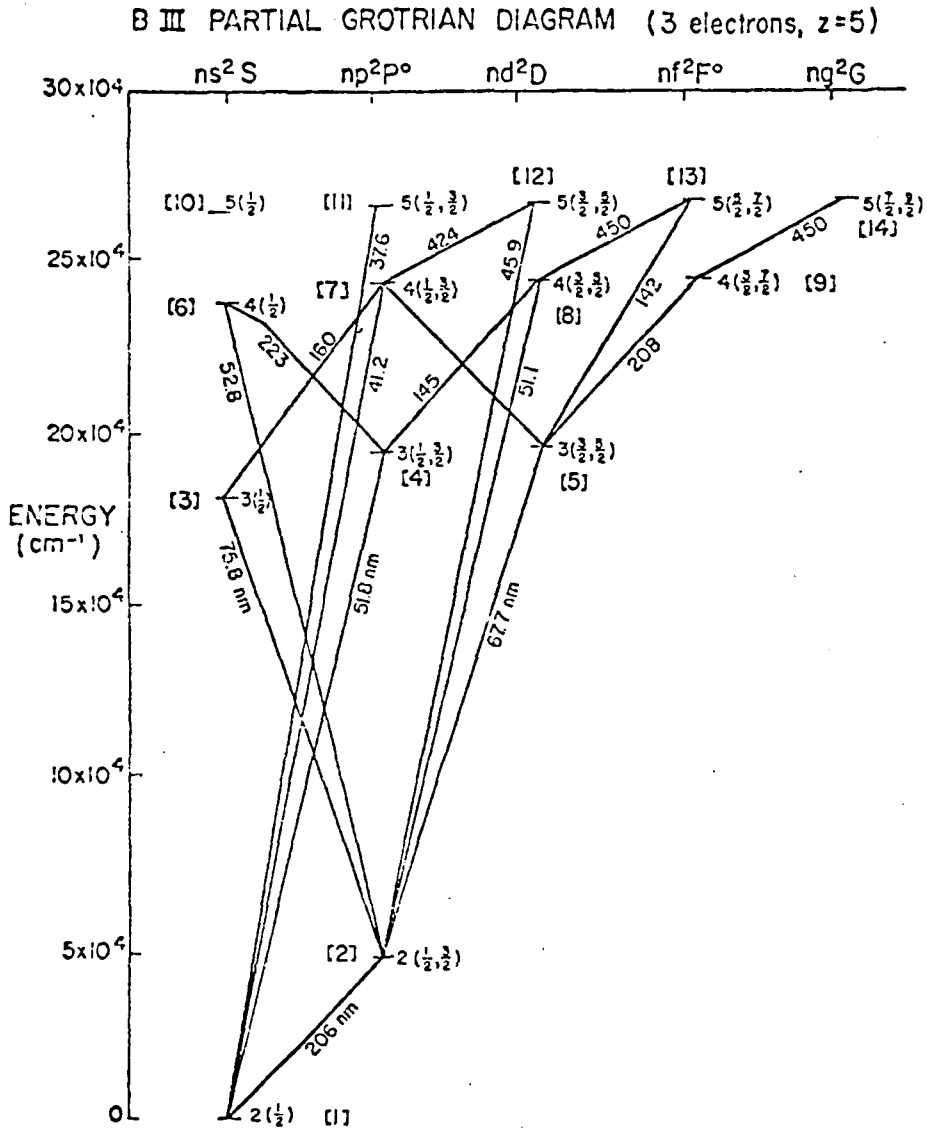
B III PARTIAL GROTRIAN DIAGRAM (3 electrons, z=5)
ns² S
np²P°
nd²D
nf²F°
ng²G
ENERGY (cm⁻¹)
30x10⁴
25x10⁴
20x10⁴
15x10⁴
10x10⁴
5x10⁴
0
[1]
[2]
[3]
[4]
[5]
[6]
[7]
[8]
[9]
[10]
[11]
[12]
[13]
[14]
206 nm
515.8 nm
627 nm
759 nm
52.8
223
160
37.6
424
41.2
145
45.9
511
450
142
208
450

FIG.3

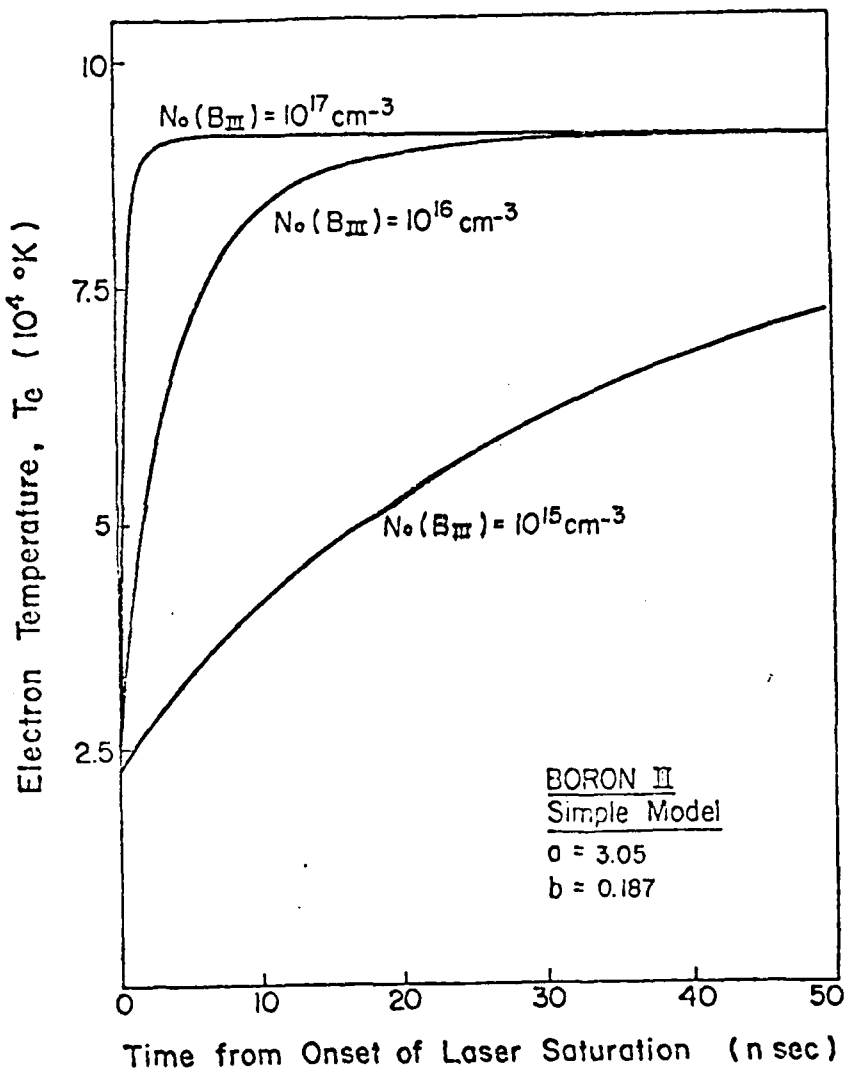
Electron Temperature, Te (10⁴ °K)
Time from Onset of Laser Saturation (n sec)
No(BIII) = 10¹⁷ cm⁻³
No(BIII) = 10¹⁶ cm⁻³
No(BIII) = 10¹⁵ cm⁻³
BORON II
Simple Model
a = 3.05
b = 0.187
10
7.5
5
2.5
0
10
20
30
40
50

FIG.4

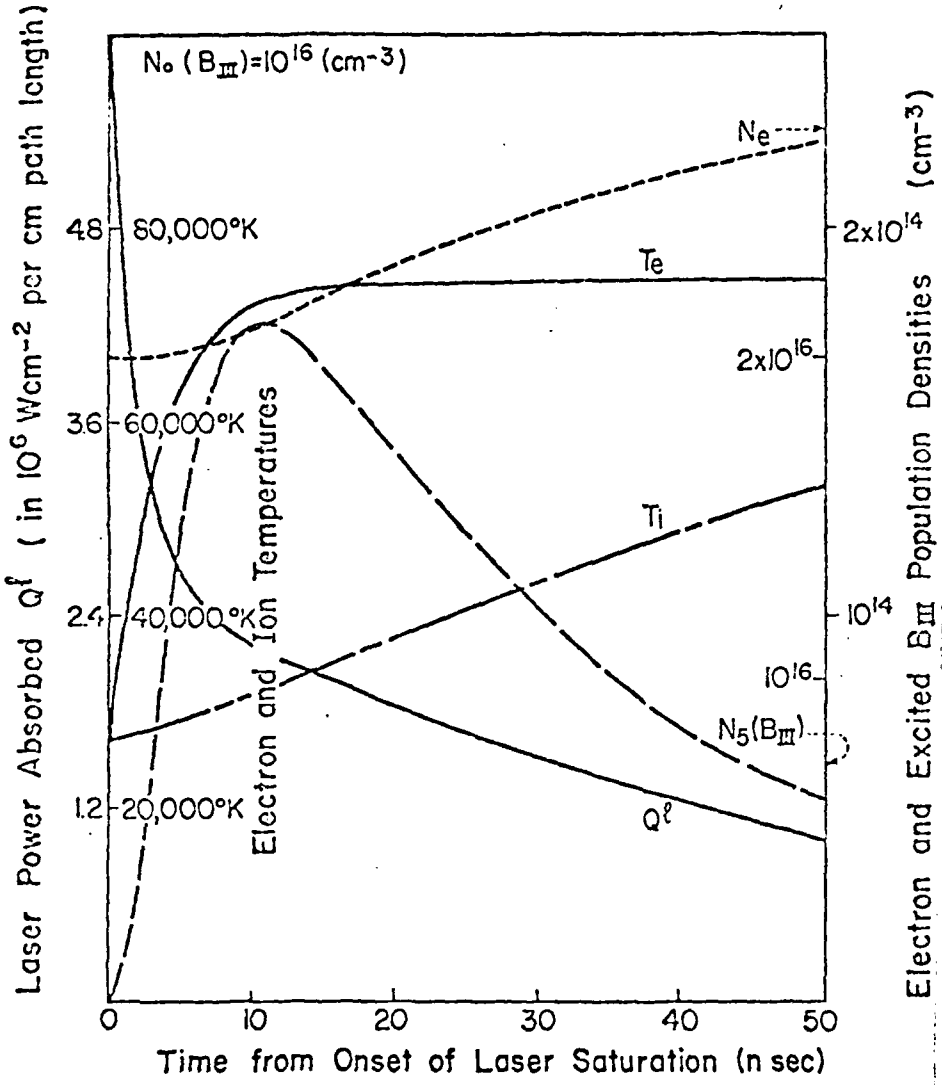
$N_o(B_{III})=10^{16}$ (cm^{-3})
N_e
80,000°K
T_e
60,000°K
T_i
40,000°K
20,000°K
Q^ℓ
$N_5(B_{III})$
Laser Power Absorbed Q^ℓ (in 10^6 Wcm^{-2} per cm path length)
Electron and Ion Temperatures
Electron and Excited B_{III} Population Densities (cm^{-3})
4.8
3.6
2.4
1.2
2×10^{14}
2×10^{16}
10^{14}
10^{16}
0
10
20
30
40
50
Time from Onset of Laser Saturation (n sec)

FIG 5

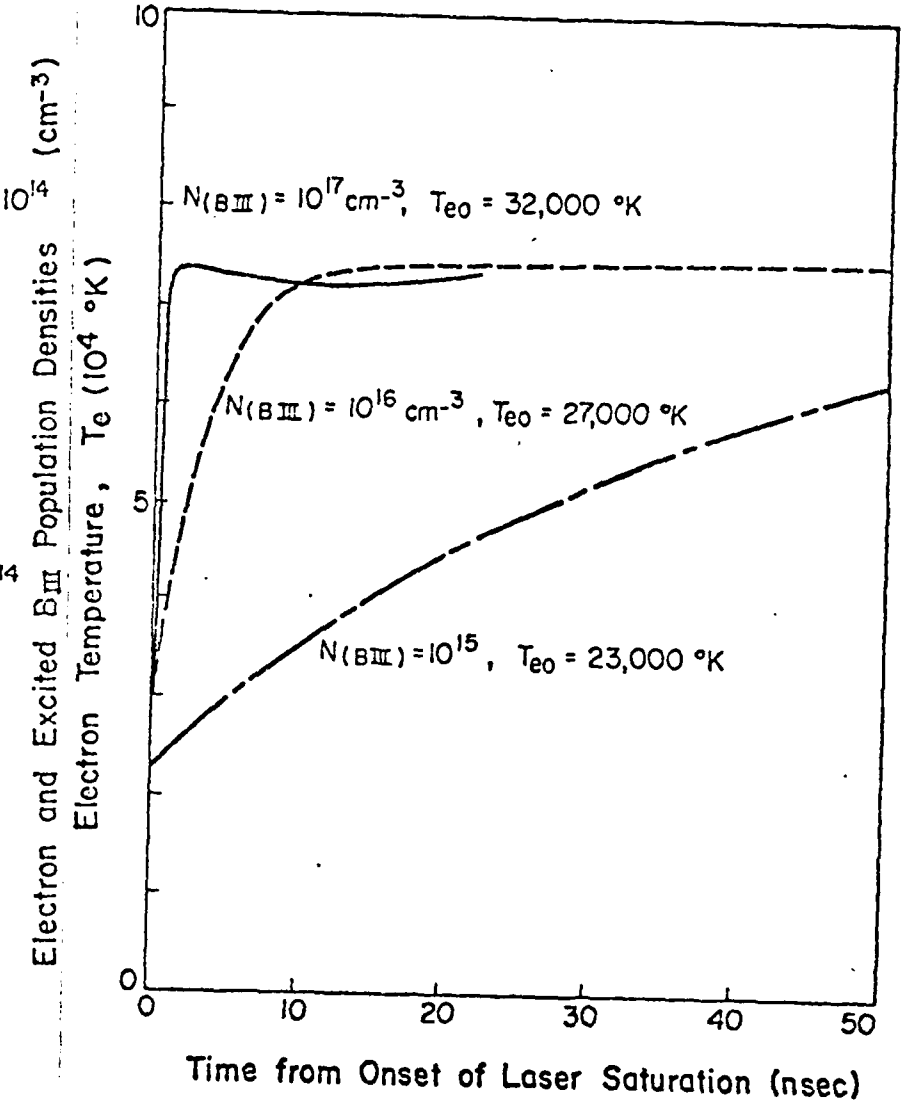
$N(B_{III}) = 10^{17}$cm^{-3}, T_{eo} = 32,000 °K
$N(B_{III}) = 10^{16}$ cm^{-3}, T_{eo} = 27,000 °K
$N(B_{III}) = 10^{15}$, T_{eo} = 23,000 °K
Electron and Excited B_{III} Population Densities
Electron Temperature, T_e (10^4 °K)
10
5
0
0
10
20
30
40
50
Time from Onset of Laser Saturation (nsec)

FIG 6